Higgs scalar potential coupled to gravity in the exponential parametrization in arbitrary gauge

Nobuyoshi Ohta[1,2,*] and Masatoshi Yamada[3,†]

[1]*Department of Physics, National Central University, Zhongli, Taoyuan 320317, Taiwan*
[2]*Research Institute for Science and Technology, Kindai University, Higashi-Osaka, Osaka 577-8502, Japan*
[3]*Institut für Theoretische Physik, Universität Heidelberg, D-69120 Heidelberg, Germany*

(Received 21 October 2021; accepted 22 December 2021; published 12 January 2022)

We study the parametrization and gauge dependences in the Higgs field coupled to gravity in the context of asymptotic safety. We use the exponential parametrization to derive the fixed points for the cosmological constant, Planck mass, Higgs mass and its coupling, keeping arbitrary gauge parameters α and β, and compare the results with the linear split. We find that the beta functions for the Higgs potential are expressed in terms of redefined Planck mass such that the apparent gauge dependence is absent. Only the trace mode of the gravity fluctuations couples to the Higgs potential and it tends to decouple in the large β limit, but the anomalous dimension becomes large, invalidating the local potential approximation. This gives the limitation of the exponential parametrization. There are also singularities for some values of the gauge parameters but well away from these, we find rather stable fixed points and critical exponents. We thus find that there are regions for the gauge parameters to give stable fixed points and critical exponents against the change of gauge parameters. The Higgs coupling is confirmed to be irrelevant for the reasonable choice of gauge parameters.

DOI: 10.1103/PhysRevD.105.026013

I. INTRODUCTION

The functional renormalization group [1–6] is a powerful method to tackle nonperturbative phenomena in quantum field theory. For reviews, see Refs. [7–17]. Its application to gauge theories has elucidated the nonperturbative nature of gauge theories [13,18–26]. In particular, the functional renormalization group has contributed towards asymptotically safe quantum gravity [27–29] which is formulated as a nonperturbative quantum field theory. Its recent developments are summarized in Refs. [30–42]. A central object in the functional renormalization group is the effective average action Γ_k and its second-order functional derivative $\Gamma_k^{(2)}$ whose inverse form corresponds to the full propagator, so that in general the gauge fixing is required for the gauge field propagator in addition to the ultraviolet (UV) regularization.

Physical quantities should depend on neither gauge fixing parameters nor regularization schemes; however, such an independence may be easily destroyed by the gauge fixing and approximations in the quantum theory. Therefore, we need to carefully handle their dependence when we apply the functional renormalization group especially to gauge systems. Good gauge choice may be identified by allowing for a family of gauge and identifying stationary points in the parameter space. This is the principle of minimum sensitivity advocated in Refs. [43–45].

Recently the effective potential for the Higgs field was calculated in various works [46–55]. It is an important quantity to understand the electroweak symmetry breaking in the Standard Model of particle physics. The fixed points of the quantum effective potential for the Higgs field was studied by calculating beta functions of the couplings in the theory, and it has been shown that quartic self-interaction of the Higgs scalar field is an irrelevant coupling at the asymptotically safe UV fixed point of quantum gravity. This has an important prediction to the ratio of the masses of the Higgs boson and top quark [53,54,56–60]. Moreover, the understanding of the energy scaling of the Higgs mass parameter is essential towards the gauge hierarchy problem. It was pointed out in Ref. [61] that quantum-gravity fluctuations make the Higgs mass parameter irrelevant and thus could play a key role for solving the gauge hierarchy problem. The determination whether the number of the relevant coupling constants is finite and how many

*ohtan@ncu.edu.tw
†m.yamada@thphys.uni-heidelberg.de

are there are also crucial questions for obtaining predictable theory of quantum gravity. By including higher curvature terms [62–66], these problems have been studied in pure gravity [67–73]. Extensions to matter system including standard model of particle physics and beyond are considered [53,74–79]. See also Refs. [80–82] as applications of the asymptotic safety scenario for gravity-matter systems.

Although these works represent important progress, it is also known to suffer from the gauge dependence in the gravity contribution [83–85]. The question arises then how much the obtained results are reliable in the physics of spontaneous breaking of the symmetry. We would like to study this problem by keeping the gauge parameters, and check how much the results depend on them.

Another possible problem is that it is found that there appears some unphysical poles in the cosmological constant in the beta functions for the gravity couplings if one uses the linear parametrization of the metric

$$g_{\mu\nu} = \bar{g}_{\mu\nu} + h_{\mu\nu}. \tag{1.1}$$

Because of this, it appears the results are unstable close to the singularity. It is possible that the sign of the critical exponents changes near the singularity, and thus drastically changes the nature of the fixed points [53]. This might be a signal of phase transition, but this cannot be treated in the polynomial truncation. In the present setting, it would be better to consider the region away from the singularity. In this respect, it is known that such singularity in the cosmological constant does not appear if one uses the exponential parametrization for the gravitational fluctuation [49]:

$$g_{\mu\nu} = \bar{g}_{\mu\lambda}(e^h)^\lambda{}_\nu = \bar{g}_{\mu\nu} + h_{\mu\nu} + \frac{1}{2}h_{\mu\lambda}h^\lambda_\nu + O(h^3). \tag{1.2}$$

The parametrization was first used in Ref. [86], applied to $D = 4$ gravity in asymptotic safety [87–89] and later generalized to more general parametrization to study various parametrization dependence [45,90–93]. Here we choose this exponential parametrization in order to avoid the unphysical singularity and check the consistency with the earlier results. This parametrization has also the advantage that the resulting beta function does not depend on the gauge choice [94,95]. However we will find that this parametrization also has some problem in the local potential approximation.

In this work, using the Wetterich equation [4], we study the parametrization and gauge dependences of the fixed point structure and the critical exponents in the Higgs-gravity system by comparing the results with the exponential (1.2) and linear (1.1) parametrizations with arbitrary gauge parameters, and check if we can find reasonable results despite these dependences. It turns out that if we use a redefined Planck mass, the beta functions for the scalar potential in the exponential parametrization become independent of the gauge parameters, and we can discuss the fixed points without apparent gauge dependence. This is an advantage of the exponential parametrization, but the price is that the anomalous dimension of the Higgs scalar becomes large in general. However we have found that its effect is actually not so big owing to the suppression factor like $1/4$. We have found that there is a reasonable range of gauge parameters which give stable results against change of the parameters. Relying on the principle of minimal sensitivity, we conclude that the coupling of the self-interaction of the Higgs field is irrelevant.

This paper is organized as follows: In Sec. II, we introduce the effective action for the Higgs-gravity system with two arbitrary gauge parameters. The two-point functions, i.e., the Hessians, are also derived. The explicit forms of the beta functions for the Higgs-gravity system are derived with the full dependence on the gauge parameters in Sec. III. The anomalous dimension for the Higgs scalar is also given. In Sec. IV, we discuss the fixed points and critical exponents in the exponential parametrization for various choices of the gauge parameters, and comparae the results in the linear parametrization. In Sec. V, we further study the gauge parameter dependence of the fixed points and anomalous dimensions. Section VI is devoted to the summary of our results and conclusions. Technical details of the calculations and definitions are relegated to Appendixes. In Appendix A, we give the York decomposition and discuss the Jacobian which arises in changing the variables. In Appendix B, we give the definition and properties of the Lichnerowicz Laplacians. Some technicality in the variation of the action is summarized in Appendix C. The flow equations and anomalous dimension of the Higgs field are calculated in Appendix D.

II. ACTION AND HESSIANS

A. Gauge fixed action for the Higgs coupled to gravity

We would like to calculate the beta functions for Higgs couplings, the Newton constant, and cosmological constant with arbitrary gauge fixing parameters, in order to check gauge dependence explicitly. The effective action we consider is given by

$$\Gamma_k = \Gamma^{\text{gravity}} + \Gamma^{\text{Higgs}}. \tag{2.1}$$

The gravity part Γ^{gravity} consists of the Einstein-Hilbert term, gauge fixing, and Faddeev-Popov ghost terms given by

$$\begin{aligned}
\Gamma^{\text{gravity}} &= -Z_N \int d^4x\sqrt{g}R + \Gamma_{\text{GF}} + \Gamma_{\text{gh}},\\
\Gamma_{\text{GF}} &= \frac{1}{2\alpha}\int d^4x\sqrt{\bar{g}}\bar{g}^{\mu\nu}f_\mu f_\nu,\\
\Gamma_{\text{gh}} &= \int d^dx\sqrt{\bar{g}}\bar{C}_\mu\left(\bar{\nabla}^2\delta^\mu_\nu + \frac{1-\beta}{2}\bar{\nabla}^\mu\bar{\nabla}_\nu + \bar{R}^\mu_\nu\right)C^\nu,
\end{aligned} \tag{2.2}$$

where $Z_N = 1/(16\pi G)$, $\bar{g} = \det(\bar{g}_{\mu\nu})$, α and β are (dimensionful and dimensionless) gauge fixing parameters, and the gauge fixing function f_μ is

$$f_\mu = \bar{\nabla}^\nu h_{\mu\nu} - \frac{1+\beta}{4}\bar{\nabla}_\mu h. \tag{2.3}$$

Here the full metric is split into background $\bar{g}_{\mu\nu}$ and fluctuation $h_{\mu\nu}$ by the exponential parametrization (1.2) and $h = \bar{g}^{\mu\nu}h_{\mu\nu} = h^\nu{}_\nu$ is the trace mode in the fluctuation field. The covariant derivative ∇_μ is a general relativity metric covariant derivative constructed using the Levi-Civita connection, and the barred one is constructed with the background metric. We keep both the gauge parameters α and β arbitrary in the following analysis in order to study the gauge dependence of the results.

The Higgs field is a component of the doublet field coupled to the $SU(2)_L$ and $U(1)_Y$ gauge fields as well as to quarks and leptons. The contributions from those fields to the beta function are smaller than the ones from the graviton near the UV fixed point, and we can safely restrict the discussions to a single scalar field with $\mathbb{Z}_2$ symmetry. The action for the Higgs field is

$$\Gamma^{\rm Higgs} = \int d^4x\sqrt{g}\left[\frac{Z_\phi}{2}g^{\mu\nu}\partial_\mu\phi\partial_\nu\phi + U(\rho)\right], \tag{2.4}$$

where the effective potential is assumed to depend only on the invariant $\rho = \phi^2/2$.

To derive the flow equations in the system (2.1), we use the Wetterich equation [4] whose form reads

$$\partial_t\Gamma_k = \frac{1}{2}{\rm Tr}[(\Gamma_k^{(2)} + \mathcal{R}_k)^{-1}\partial_t\mathcal{R}_k], \tag{2.5}$$

with $t = \log k$ the dimensionless scale. Here, $\mathcal{R}_k$ is a regulator function and $\Gamma_k^{(2)}$ is the full two-point function, i.e., the so-called Hessian. In the next section, we show the Hessians for the effective action (2.1).

B. Hessians

We consider the theory on the Einstein space in which the Ricci tensor is given by

$$\bar{R}_{\mu\nu} = \frac{\bar{R}}{4}\bar{g}_{\mu\nu}. \tag{2.6}$$

Using the York decomposition described in Appendix A, we can read off the Hessian for the gravity from, for example, [88][1]:

$$I^{\rm gravity(2)} = Z_N\left[\frac{1}{4}h^{TT}_{\mu\nu}\left(\Delta_{L2} - \frac{\bar{R}}{2}\right)h^{TT,\mu\nu} - \frac{3}{32}\sigma\Delta_{L0}^2\left(\Delta_{L0} - \frac{\bar{R}}{3}\right)\sigma - \frac{3}{16}h\Delta_{L0}\left(\Delta_{L0} - \frac{\bar{R}}{3}\right)\sigma - \frac{3}{32}h\left(\Delta_{L0} + \frac{\bar{R}}{3}\right)h\right]. \tag{2.7}$$

Here, Δ_{Li} are the Lichnerowicz Laplacians defined in Appendix B, and hereafter we drop the bars on the covariant derivatives and Lichnerowicz Laplacians. We will rescale the graviton fields as $h_{\mu\nu} \to Z_N^{-1/2}h_{\mu\nu}$ so that we can get rid of this factor from the Hessian, though it will appear in other terms. Note that in the exponential parametrization, the gauge mode ξ_μ completely decouples from the gauge invariant action. The gauge fixing term then reduces to

$$I_{\rm GF} = \frac{1}{2\tilde{\alpha}}\int d^4x\left[\xi_\mu\left(\Delta_{L1} - \frac{\bar{R}}{2}\right)^2\xi^\mu + \frac{9}{16}\sigma\Delta_{L0}\left(\Delta_{L0} - \frac{\bar{R}}{3}\right)^2\sigma + \frac{3\beta}{8}\sigma\Delta_{L0}\left(\Delta_{L0} - \frac{\bar{R}}{3}\right)h + \frac{\beta^2}{16}h\Delta_{L0}h\right], \tag{2.8}$$

where $\tilde{\alpha} = Z_N\alpha$ is the dimensionless gauge fixing parameter.

The Faddeev-Popov ghost is decomposed as

$$C^\mu = C^{T\mu} + \nabla^\mu\frac{1}{\sqrt{\Delta_{L0}}}C^L, \tag{2.9}$$

with $\nabla_\mu C^{T\mu} = 0$, and the same for $\bar{C}_\mu$. The ghost action reduces to

$$\Gamma_{\rm gh} = \int d^4x\sqrt{\bar{g}}\left[-\bar{C}^T_\mu\left(\Delta_{L1} - \frac{\bar{R}}{2}\right)C^{T\mu} - \frac{3-\beta}{2}\bar{C}^L\left(\Delta_{L0} - \frac{\bar{R}}{3-\beta}\right)C^L\right]. \tag{2.10}$$

Since we are interested in the corrections to the Higgs potential, we neglect those terms where the derivatives are acting on the (background) scalar fields. The Higgs contribution is then

$$I^{(2)}_{\rm Higgs} = \varphi\left[\frac{Z_\phi}{2}\Delta_{L0} + \frac{1}{2}(U' + 2U''\rho)\right]\Big|_{\phi=\bar{\phi}}\varphi + \frac{1}{2}Z_N^{-1/2}hU'\varphi + \frac{1}{8}Uh^2, \tag{2.11}$$

where the prime is the derivative with respect to ρ, and $\bar{\phi}$ and φ are background and fluctuation fields of ϕ, respectively. Note that only the trace mode of the gravity fluctuation couples to the Higgs potential in the exponential parametrization.

[1]There are typos in the last terms in Eqs. (2.8) and (2.9) in Ref. [88]; the factor should be 1 instead of 2.

The Hessian for the transverse-traceless (TT) mode is given by

$$\frac{1}{2}h^{TT,\mu\nu}\Gamma^{TT}_{\mu\nu,\alpha\beta}h^{TT,\alpha\beta}, \qquad \Gamma^{TT}_{\mu\nu,\alpha\beta}=\frac{1}{2}\left(\Delta_{L2}-\frac{\bar{R}}{2}\right)E_{\mu\nu\alpha\beta}, \tag{2.12}$$

with the unity matrix $E_{\mu\nu\alpha\beta}=\frac{1}{2}(\bar{g}_{\mu\alpha}\bar{g}_{\nu\beta}+\bar{g}_{\mu\beta}\bar{g}_{\nu\alpha})$. The Hessian for the spin-1 transverse mode comes only from the gauge fixing term (2.8) and is given by

$$\frac{1}{2}\xi^{\mu}\Gamma^{\xi\xi}_{\mu,\nu}\xi^{\nu}, \qquad \Gamma^{\xi\xi}_{\mu,\nu}=\left(\Delta_{L1}-\frac{\bar{R}}{2}\right)^2\bar{g}_{\mu\nu}, \tag{2.13}$$

after the rescaling $\xi_\mu\to\sqrt{\tilde{\alpha}}\xi_\mu$. In the (σ,h,φ) basis, the Hessian for spin-0 scalar modes becomes

$$\frac{1}{2}\begin{pmatrix}\sigma & h & \varphi\end{pmatrix}\Gamma^S\begin{pmatrix}\sigma\\ h\\ \varphi\end{pmatrix} \equiv\frac{1}{2}\begin{pmatrix}\sigma & h & \varphi\end{pmatrix}\begin{pmatrix}\Gamma_{\sigma\sigma} & \Gamma_{\sigma h} & \Gamma_{\sigma\phi}\\ \Gamma_{h\sigma} & \Gamma_{hh} & \Gamma_{h\phi}\\ \Gamma_{\phi\sigma} & \Gamma_{\phi h} & \Gamma_{\phi\phi}\end{pmatrix}\begin{pmatrix}\sigma\\ h\\ \varphi\end{pmatrix}, \tag{2.14}$$

where

$$\Gamma^S=\begin{pmatrix}-\frac{3}{16}(\Delta_{L0})^2(\Delta_{L0}-\frac{\bar{R}}{3}) & -\frac{3}{16}\Delta_{L0}(\Delta_{L0}-\frac{\bar{R}}{3}) & 0\\ -\frac{3}{16}\Delta_{L0}(\Delta_{L0}-\frac{\bar{R}}{3}) & -\frac{3}{16}(\Delta_{L0}+\frac{\bar{R}}{3})+\frac{1}{4}Z_N^{-1}U & \frac{1}{2}Z_N^{-1/2}U'\sqrt{2\bar{\rho}}\\ 0 & \frac{1}{2}Z_N^{-1/2}U'\sqrt{2\bar{\rho}} & Z_\phi\Delta_{L0}+M_H^2(\bar{\rho})\end{pmatrix} +\frac{1}{\tilde{\alpha}}\begin{pmatrix}\frac{9}{16}\Delta_{L0}(\Delta_{L0}-\frac{\bar{R}}{3})^2 & \frac{3\beta}{16}\Delta_{L0}(\Delta_{L0}-\frac{\bar{R}}{3}) & 0\\ \frac{3\beta}{16}\Delta_{L0}(\Delta_{L0}-\frac{\bar{R}}{3}) & \frac{\beta^2}{16}\Delta_{L0} & 0\\ 0 & 0 & 0\end{pmatrix}, \tag{2.15}$$

where we have defined the effective Higgs scalar mass

$$M_H^2(\bar{\rho})=U'(\bar{\rho})+2U''(\bar{\rho})\bar{\rho}. \tag{2.16}$$

There are also determinants that have to be taken into account coming from changing field variables in the York decomposition:

$$\mathrm{Det}_{(1)}\left(\Delta_{L1}-\frac{\bar{R}}{2}\right)^{1/2}\mathrm{Det}_{(0)}\left[\Delta_{L0}\left(\Delta_{L0}-\frac{\bar{R}}{3}\right)\right]^{1/2} \equiv J_{\mathrm{grav1}}J_{\mathrm{grav0}}. \tag{2.17}$$

See Appendix A for the derivation of this Jacobian.

Let us here consider properties of the fields appearing in our Hessian. We first note that the scalar part in the gravity Hessian (2.7) can be written as

$$-\frac{3}{32}s\left(\Delta_{L0}-\frac{\bar{R}}{3}\right)s-\frac{\bar{R}}{16}h^2, \tag{2.18}$$

where

$$s=\Delta_{L0}\sigma+h, \tag{2.19}$$

is the gauge-invariant variable. On the other hand, if we use the York decomposition, our gauge fixing function (2.3) on the Einstein space (2.6) becomes

$$f_\mu=-\left(\Delta_{L1}-\frac{\bar{R}}{2}\right)\xi_\mu-\nabla_\mu\left[\frac{3}{4}\left(\Delta_{L0}-\frac{\bar{R}}{3}\right)\sigma+\frac{\beta}{4}h\right]. \tag{2.20}$$

We see that for the choice of $\beta=3$, the scalar combination in this gauge fixing function becomes precisely the gauge invariant variable s modulo curvature term. We will see that there is a singularity at $\beta=3$ in various quantities in the following. The origin of this singular behavior is that the longitudinal direction of the metric fluctuation is not affected by the gauge fixing [45,90,91]. In other words, the scalar modes in the gauge fixing function become exactly the gauge-invariant combination and it does not fix the gauge for this value of β. We also see related singularity in the longitudinal mode of the ghost field (2.10).

The gauge fixing function can be written as

$$f_\mu=-\left(\Delta_{L1}-\frac{\bar{R}}{2}\right)\xi_\mu-\frac{3-\beta}{4}\nabla_\mu\left(\Delta_{L0}-\frac{\bar{R}}{3-\beta}\right)\chi, \tag{2.21}$$

where

$$\chi=\frac{(3\Delta_{L0}-\bar{R})\sigma+\beta h}{(3-\beta)\Delta_{L0}-\bar{R}} \tag{2.22}$$

is a new degree of freedom. We find that χ transforms as σ. In the absence of matter, the last term in Eq. (2.18) is zero on shell, and the Hessian for gravity is written entirely in terms of the gauge-invariant variables h^{TT} and s, and the

gauge fixing is entirely in terms of the gauge-variant fields ξ and χ. If we consider $\beta \to \infty$, we have $h = -\Delta_{L0}\chi$, and the gauge fixing strongly enforces the condition $\chi = 0$, independently of α. This practically kills h, and setting $\alpha = 0$ removes the gauge-variant field ξ, and then we have only the contributions from gauge-invariant variables. Since this choice sets $h = 0$, this is called a unimodular physical gauge [49,88]. So the gauge choice $\alpha = 0$, $\beta = \infty$ may be an interesting physical gauge. Moreover, it is known that singularities in propagators of the metric fluctuation fields disappear in the pure gravity. However, in the presence of scalar fields, we have seen that only the trace mode of the metric fluctuation makes a contribution to the scalar potential, which vanishes in the $\beta = \infty$ limit. This implies that the metric fluctuations contribute only to Z_ϕ in this limit.

Another particular choice for the gauge fixing parameters may be $\tilde{\alpha} \to 0$ and $\beta = -1$ [54,55,96,97]. For this choice, the gauge-variant modes ξ_μ and χ are removed by the gauge fixing and then the TT mode and the gauge invariant scalar modes (2.19) remain as physical modes.

Note also that the choice $\tilde{\alpha} \to 0$ and $\beta = 0$ is often employed. In this gauge fixing, $\beta = 0$ keeps only $(\Gamma^{(2)}_{\rm GF})_{\sigma\sigma}$ which gives the kinetic term of the σ mode in the Landau gauge $\tilde{\alpha} \to 0$ [see Eq. (2.15)] and thus the structure of the flow equations becomes simple.

III. FLOW EQUATIONS

The flow equation for the system (2.1) can be schematically written as

$$\partial_t \Gamma_k = \frac{1}{2}\mathrm{Tr}\frac{\partial_t \mathcal{R}_k}{\Gamma^{(2)}_k + \mathcal{R}_k}\bigg|_{h^{TT}h^{TT}} + \frac{1}{2}\mathrm{Tr}\frac{\partial_t \mathcal{R}_k}{\Gamma^{(2)}_k + \mathcal{R}_k}\bigg|_{\xi\xi} - \mathrm{Tr}\frac{\partial_t \mathcal{R}_k}{\Gamma^{(2)}_k + \mathcal{R}_k}\bigg|_{C^T C^T} - \frac{1}{2}\mathrm{Tr}\frac{\partial_t \mathcal{R}_k}{\Gamma^{(2)}_k + \mathcal{R}_k}\bigg|_{J_{\rm grav1}} + \frac{1}{2}\mathrm{Tr}\frac{\partial_t \mathcal{R}_k}{\Gamma^{(2)}_k + \mathcal{R}_k}\bigg|_{\rm scalar} - \mathrm{Tr}\frac{\partial_t \mathcal{R}_k}{\Gamma^{(2)}_k + \mathcal{R}_k}\bigg|_{C^L C^L} - \frac{1}{2}\mathrm{Tr}\frac{\partial_t \mathcal{R}_k}{\Gamma^{(2)}_k + \mathcal{R}_k}\bigg|_{J_{\rm grav0}}. \tag{3.1}$$

Here we employ the regulator such that Lichnerowicz Laplacians are replaced by $P_k = \Delta_L + R_k(\Delta_L)$, i.e.,

$$\mathcal{R}_k(\Delta_L) = \Gamma^{(2)}_k(P_k) - \Gamma^{(2)}_k(\Delta_L). \tag{3.2}$$

In this work, the flow generators in Eq. (3.1) are calculated using the optimized cutoff [98]

$$R_k(\Delta_L) = (k^2 - \Delta_L)\theta(k^2 - \Delta_L). \tag{3.3}$$

In the calculation of the contributions of the spin-0 part, we should use the matrix form to take into account the mixing terms.

We define the dimensionless quantities by

$$\tilde{U}(\tilde{\rho}) = \frac{U(\bar{\rho})}{k^4}, \qquad \tilde{\rho} = \frac{Z_\phi \bar{\rho}}{k^2}, \tag{3.4}$$

as well as the dimensionless ratio

$$v(\tilde{\rho}) = \frac{2U(\bar{\rho})}{M_P^2 k^2} = \frac{2\tilde{U}(\tilde{\rho})}{\tilde{M}_P^2}, \tag{3.5}$$

where the Planck mass and its dimensionless version are defined by

$$M_P^2 = 2Z_N, \qquad \tilde{M}_P^2 = \frac{M_P^2}{k^2}. \tag{3.6}$$

We find the flow equation for the dimensionless effective scalar potential

$$\partial_t \tilde{U}(\tilde{\rho}) = -4\tilde{U}(\tilde{\rho}) + (2 + \eta_\phi)\tilde{\rho}\partial_{\tilde{\rho}}\tilde{U}(\tilde{\rho}) + \frac{1}{16\pi^2}\ell_0^4(0) + \frac{1}{16\pi^2}\ell_0^4(-\tilde{M}_s^2(\tilde{\rho})) + \frac{1}{8\pi^2}\left(1 - \frac{\eta_\phi}{6}\right)\left[1 - 2\frac{4(3-\tilde{\alpha})}{(3-\beta)^2\tilde{M}_P^2}\tilde{U}(\tilde{\rho})\right]\ell_0^4(-\tilde{M}_s^2(\tilde{\rho}))\ell_0^4(\tilde{M}_H^2(\tilde{\rho})), \tag{3.7}$$

where η_ϕ is the anomalous dimension of ϕ:

$$\eta_\phi = -\frac{\partial_t Z_\phi}{Z_\phi}. \tag{3.8}$$

Details of the derivation are given in Appendix D. Here $\tilde{M}_H^2(\tilde{\rho})$ is the dimensionless version of the Higgs mass in Eq. (2.16) and we have also defined a $\tilde{\rho}$-dependent mass of scalar modes in the metric fluctuations:

$$\tilde{M}_s^2(\tilde{\rho}) = \frac{4(3-\tilde{\alpha})}{(3-\beta)^2\tilde{M}_P^2}\left[2\tilde{U}(\tilde{\rho}) - \frac{4\tilde{\rho}(U'(\tilde{\rho}))^2}{1+\tilde{M}_H^2(\tilde{\rho})}\right]. \tag{3.9}$$

We have further introduced the shorthand threshold function

$$\ell_p^{2n}(x) = \frac{1}{n!}\frac{1}{(1+x)^{p+1}}. \tag{3.10}$$

This function originates from loop integrals in the heat kernel expansion. See Appendix D 1 for the precise definition.

Next, we expand the potential in polynomials of $\tilde{\rho}$ around the origin $\tilde{\rho} = 0$:

$$\tilde{U}(\tilde{\rho}) = \tilde{V} + \tilde{m}_H^2\tilde{\rho} + \frac{\tilde{\lambda}}{2}\tilde{\rho}^2 + \cdots, \tag{3.11}$$

where $\tilde{m}_H^2 = M_H^2(\bar{\rho}=0)/k^2$. Note that $\tilde{V}$ corresponds to the cosmological constant by $2\tilde{\Lambda} = 16\pi\tilde{G}_N\tilde{V} = \frac{2\tilde{V}}{\tilde{M}_P^2}$. From this expansion (3.11), we define the $\tilde{\rho}$-independent part of Eq. (3.5) and Eq. (3.9), respectively, by

$$v_0 = \frac{2\tilde{V}}{\tilde{M}_P^2}, \qquad \tilde{m}_s^2 = \frac{4(3-\tilde{\alpha})}{(3-\beta)^2}v_0 = \left(\frac{4(3-\tilde{\alpha})}{(3-\beta)^2\tilde{M}_P^2}\right)2\tilde{V}, \tag{3.12}$$

We find the beta functions for each coupling in the scalar potential (3.11) as follows:

$$\partial_t\tilde{V} = -4\tilde{V} + \frac{1}{16\pi^2}\left[\ell_0^4(0) + \ell_0^4(-\tilde{m}_s^2) + \left(1-\frac{\eta_\phi}{6}\right)\ell_0^4(\tilde{m}_H^2)\right], \tag{3.13}$$

$$\begin{aligned}\partial_t\tilde{m}_H^2 = {}& (-2+\eta_\phi+A)\tilde{m}_H^2 - \left(1-\frac{\eta_\phi}{6}\right)\frac{3\tilde{\lambda}}{32\pi^2}\ell_1^2(\tilde{m}_H^2) \\ & - \frac{\tilde{m}_H^4}{8\pi^2}\frac{4(3-\tilde{\alpha})}{(3-\beta)^2\tilde{M}_P^2}\left[\ell_1^2(-\tilde{m}_s^2)\ell_0^2(\tilde{m}_H^2) + \left(1-\frac{\eta_\phi}{6}\right)\ell_0^2(-\tilde{m}_s^2)\ell_1^2(\tilde{m}_H^2)\right],\end{aligned} \tag{3.14}$$

$$\begin{aligned}\partial_t\tilde{\lambda} = {}& (2\eta_\phi+A)\tilde{\lambda} + \left(1-\frac{\eta_\phi}{6}\right)\frac{9\tilde{\lambda}^2}{16\pi^2}\ell_2^0(\tilde{m}_H^2) + \frac{\tilde{m}_H^4}{4\pi^2}\left(\frac{4(3-\tilde{\alpha})}{(3-\beta)^2\tilde{M}_P^2}\right)^2\ell_2^0(-\tilde{m}_s^2) \\ & - \frac{2\tilde{m}_H^2\tilde{\lambda}}{4\pi^2}\frac{4(3-\tilde{\alpha})}{(3-\beta)^2\tilde{M}_P^2}\left[\ell_1^0(-\tilde{m}_s^2)\ell_0^0(\tilde{m}_H^2) + \left(1-\frac{\eta_\phi}{6}\right)\ell_0^0(-\tilde{m}_s^2)\ell_1^0(\tilde{m}_H^2)\right] \\ & - \frac{3\tilde{m}_H^4\tilde{\lambda}}{4\pi^2}\frac{4(3-\tilde{\alpha})}{(3-\beta)^2\tilde{M}_P^2}\left[\ell_1^0(-\tilde{m}_s^2)\ell_1^0(\tilde{m}_H^2) + 2\left(1-\frac{\eta_\phi}{6}\right)\ell_0^0(-\tilde{m}_s^2)\ell_2^0(-\tilde{m}_H^2)\right] \\ & - \frac{2\tilde{m}_H^6}{4\pi^2}\left(\frac{4(3-\tilde{\alpha})}{(3-\beta)^2\tilde{M}_P^2}\right)^2\left[2\ell_2^0(-\tilde{m}_s^2)\ell_0^0(\tilde{m}_H^2) + \left(1-\frac{\eta_\phi}{6}\right)\ell_1^0(-\tilde{m}_s^2)\ell_1^0(\tilde{m}_H^2)\right] \\ & + \frac{4\tilde{m}_H^8}{4\pi^2}\left(\frac{4(3-\tilde{\alpha})}{(3-\beta)^2\tilde{M}_P^2}\right)^2\left[\ell_2^0(-\tilde{m}_s^2)\ell_1^0(\tilde{m}_H^2) + \left(1-\frac{\eta_\phi}{6}\right)\ell_1^0(-\tilde{m}_s^2)\ell_2^0(\tilde{m}_H^2)\right].\end{aligned} \tag{3.15}$$

Here we have defined

$$A = -\frac{\partial}{\partial U(\bar{\rho})}(\partial_t U(\bar{\rho}))|_{\bar{\rho}=0} = \frac{1}{16\pi^2}\frac{4(3-\tilde{\alpha})}{(3-\beta)^2\tilde{M}_P^2}\ell_1^2(-\tilde{m}_s^2). \tag{3.16}$$

This quantity represents the anomalous dimension induced by the metric fluctuations contributing to the scalar potential, so hereafter we call it "the metric-induced anomalous dimension." In Appendix D 5, the anomalous dimension arising from the field renormalization of ϕ is found to be

$$\eta_\phi = \frac{5}{(4\pi)^2}\frac{1}{\tilde{M}_P^2}\ell_1^4(0) + \frac{12\tilde{\alpha}}{(4\pi)^2}\frac{1}{\tilde{M}_P^2}\ell_2^6(0) - \frac{1}{(4\pi)^2}\frac{4(3-\tilde{\alpha})}{(3-\beta)^2\tilde{M}_P^2}\left[\frac{1}{4}\ell_1^2(-\tilde{m}_s^2) - \frac{9\tilde{\alpha}(3-\beta)^2}{(3-\tilde{\alpha})^2}\ell_0^8(0)\right.$$
$$\left. + \frac{9(\tilde{\alpha}-\beta)^2}{(3-\tilde{\alpha})^2}(\ell_1^8(-\tilde{m}_s^2) + 2\ell_0^8(-\tilde{m}_s^2))\right] + \frac{6\tilde{\alpha}}{(4\pi)^2}\frac{1}{\tilde{M}_P^2}\left[\ell_1^6(0)\ell_0^2(\tilde{m}_H^2) + \left(1-\frac{\eta_\phi}{6}\right)\ell_1^6(\tilde{m}_H^2)\ell_0^2(0)\right]$$
$$+ \frac{2}{(4\pi)^2}\frac{4(3-\tilde{\alpha})}{(3-\beta)^2\tilde{M}_P^2}\left[\ell_0^2(\tilde{m}_H^2)\left(\ell_1^6(-\tilde{m}_s^2) + \frac{18(\tilde{\alpha}-\beta)}{(3-\tilde{\alpha})}(\ell_1^8(-\tilde{m}_s^2) + \ell_0^8(-\tilde{m}_s^2))\right.\right.$$
$$\left. + \frac{108(\tilde{\alpha}-\beta)^2}{(3-\tilde{\alpha})^2}(\ell_1^{10}(-\tilde{m}_s^2) + 2\ell_0^{10}(-\tilde{m}_s^2)) - \frac{108\tilde{\alpha}(3-\beta)^2}{(3-\tilde{\alpha})^2}\ell_0^{10}(0)\right)$$
$$+ \ell_1^2(\tilde{m}_H^2)\left(\left(1-\frac{\eta_\phi}{8}\right)\ell_0^6(-\tilde{m}_s^2) + \left(1-\frac{\eta_\phi}{10}\right)\frac{18(\tilde{\alpha}-\beta)}{(3-\tilde{\alpha})}\ell_0^8(-\tilde{m}_s^2)\right.$$
$$\left.\left. + \left(1-\frac{\eta_\phi}{12}\right)\left(\frac{108(\tilde{\alpha}-\beta)^2}{(3-\tilde{\alpha})^2}\ell_0^{10}(-\tilde{m}_s^2) - \frac{36\tilde{\alpha}(3-\beta)^2}{(3-\tilde{\alpha})^2}\ell_0^{10}(0)\right)\right)\right]. \tag{3.17}$$

In Fig. 1, the beta functions (3.13)–(3.15) are diagrammatically displayed. In particular, the metric-induced anomalous dimension A is generated by the one-loop diagram of scalar modes in the metric fluctuations which correspond to the fifth diagram on the rhs of $\partial_t\tilde{V}$ in Fig. 1. The second terms on the rhs of $\partial_t\tilde{m}_H^2$ and $\partial_t\tilde{\lambda}$ in Fig. 1 also produce the effects with A. For higher dimensional operators, we have commonly

$$A = \frac{\partial}{\partial\lambda_n}\left(-\frac{1}{2}\right), \tag{3.18}$$

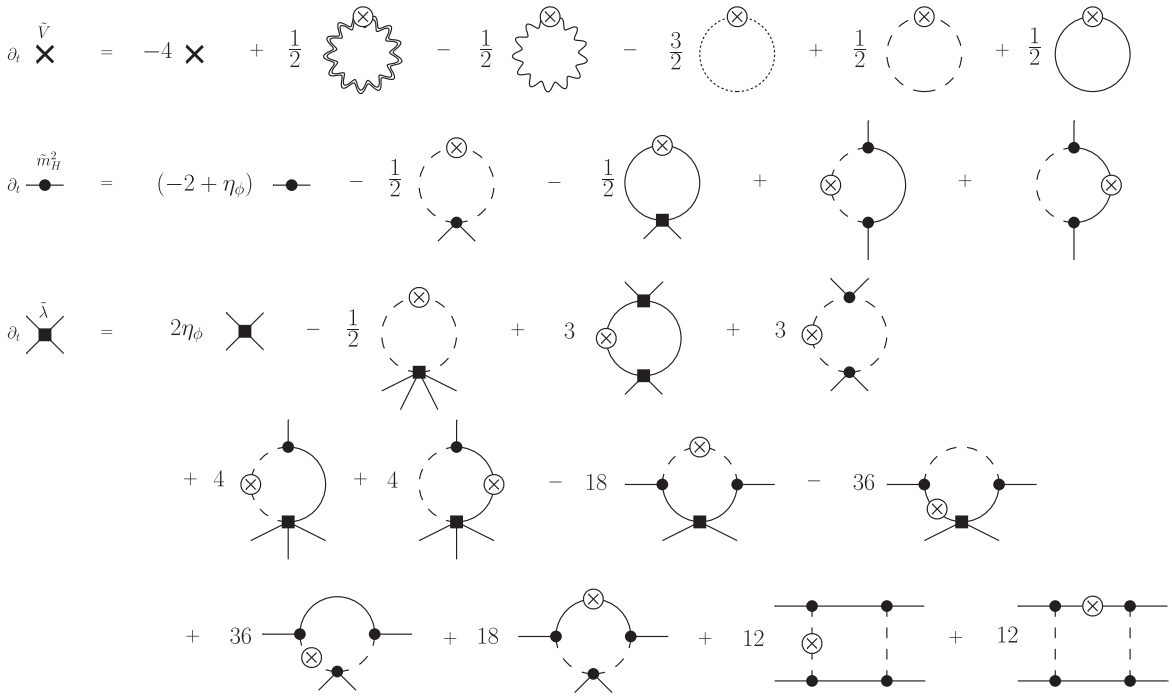

FIG. 1. Diagrammatic representation for the beta functions of the cosmological constant, the scalar mass parameter and the quartic coupling denoted by a cross, a fat dot, and a fat box, respectively. The cross circle stands for the cutoff insertion into the propagator, i.e., $\partial_t\mathcal{R}_k$. An external line is a background field $\bar{\phi}$. The double-wiggly, single-wiggly, and dashed lines are the propagators for the spin-2 TT tensor, spin-1 transverse vector and spin-0 scalar modes, respectively, while the dotted line is that of ghost fields and the Jacobians. The propagator of the scalar field fluctuation φ is drawn as a solid line.

where λ_n is a ϕ^n coupling which is denoted by a gray circle. Diagrams contributing to η_ϕ are shown in Sec. IV and Appendix D 5.

Note that if we can neglect η_ϕ and we redefine the Planck mass squared by

$$\frac{4(3-\tilde{\alpha})}{(3-\beta)^2\tilde{M}_P^2} \equiv \frac{1}{\hat{M}_P^2}, \tag{3.19}$$

the explicit dependencies on the gauge fixing parameters in the scalar potential (including the cosmological constant) disappear. Therefore, using this redefined Planck mass, we can discuss the beta functions for the scalar potential without apparent gauge dependence.

On the other hand, the beta function of the (dimensionless) Planck mass squared reads

$$\begin{aligned}\partial_t \tilde{M}_P^2 = &-2\tilde{M}_P^2 + \frac{1}{8\pi^2}\frac{13}{3}\ell_0^2(0) + \frac{1}{8\pi^2}\frac{2\beta}{3(3-\beta)}\ell_0^4(0) - \frac{1}{48\pi^2}\left(1-\frac{\eta_\phi}{4}\right)\ell_0^2(\tilde{m}_H^2) - \frac{1}{48\pi^2}\ell_0^2(-\tilde{m}_s^2) \\ &+ \frac{1}{48\pi^2}\frac{4\tilde{\alpha}-15}{3-\tilde{\alpha}} + \frac{1}{8\pi^2}\left[\frac{1}{2(3-\tilde{\alpha})} + \frac{3-\tilde{\alpha}}{(3-\beta)^2} - \frac{1}{3-\beta}\right]\ell_1^2(-\tilde{m}_s^2).\end{aligned} \tag{3.20}$$

The singularity at $\tilde{\alpha}=3$ disappears if the definition of $\tilde{m}_s^2$ given in (3.12) is substituted. However, after the replacement (3.19) is done, that singularity remains. We will discuss this issue in Sec. V. Note that since the regulators for the metric fluctuations have no dependence on M_P^2 thanks to the rescaling $h_{\mu\nu} \to Z_N^{-1/2}h_{\mu\nu}$, there is no term with the anomalous dimension $\sim\partial_t M_P^2/M_P^2$ on the rhs.

IV. LINEAR VERSUS EXPONENTIAL PARAMETRIZATION

In this section, we study the dependence of the metric-induced anomalous dimension A on the fixed-point values of the Planck mass and the cosmological constant, and the pole structure of the propagator of the metric fluctuations, in the linear and exponential parametrizations. We highlight the differences between the linear and exponential parametizations.

As pointed out in the introduction, the result using the standard linear split of the metric appears to have the problem of singularities in the cosmological constant due to poles in propagators of different modes involved in the metric fluctuations. We would like to check if we can avoid the problem in the exponential parametrization and extract physical information by comparing the results with those using the linear split. We will see that there is a pole even for the exponential parametrization in the presence of scalar fields. Such a pole is considered to signal the presence of a phase transition, and should be studied beyond polynomial truncation [8].

However, as mentioned in the previous section, the redefinition of the Planck mass (3.19) eliminates the apparent dependence of the gauge parameters from the beta function of the effective potential in the absence of η_ϕ in the exponential parametrization. Therefore, we can discuss the beta function of the Planck mass and the anomalous dimension of the scalar field without gauge dependence. When we compare the results between the linear and exponential parametrizations, we take the gauge parameters $\tilde{\alpha}=0$, $\beta=1$ (de Donder gauge) [47,53], $\tilde{\alpha}=0$, $\beta=-1$ (physical gauge) [54,55] and $\tilde{\alpha}=0$, $\beta=\infty$ (unimodular gauge) [49,87,88]. More precise analysis on the gauge dependence in the beta function of the Planck mass is presented in Sec. V.

Here we clarify a crucial difference in the contributions from the metric fluctuations to the dynamics of the scalar field between the linear and exponential parametrizations. As will be seen later, the metric-induced anomalous dimensions A and the scalar field η_ϕ play a central role in the deviation of the critical exponents of the couplings of the scalar field from their canonical scaling. Let us consider the flow equation for the two-point function of the background field $\bar{\phi}$ in a flat spacetime background $\bar{g}_{\mu\nu}=\delta_{\mu\nu}$:

$$\frac{\delta^2}{\delta\bar{\phi}(p)\delta\bar{\phi}(-p)}\partial_t\Gamma_k|_{\bar{\phi}=0} = \int d^4x[-\partial_t Z_\phi p^2 + \partial_t m_H^2]. \tag{4.1}$$

To make the discussion simple, we set $\lambda=0$.

In the exponential parametrization, the flow equations for Z_ϕ and m_H^2 are represented diagrammatically as

$\partial_t Z_\phi \sim \frac{d}{dp^2}\Big($
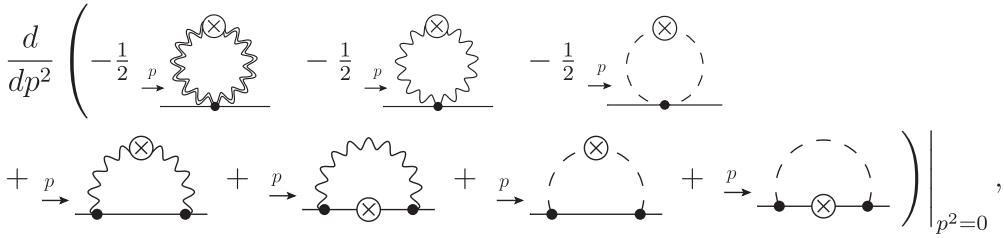
$\Big)\Big|_{p^2=0}$, (4.2)

$$\partial_t m_H^2 \sim -\tfrac{1}{2}$$ 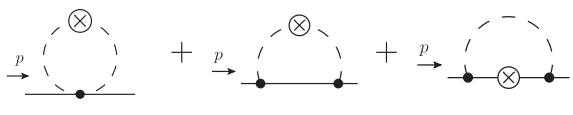 $$\Big|_{p^2=0},$$ (4.3)

where the double-wiggly, single-wiggly. and dashed lines denote the TT, spin-1 transverse vector, and spin-0 modes in the metric fluctuations, respectively, while the solid line represents the scalar field. The fat dot and cross circle stand for Z_ϕ or m_H^2 and $\partial_t \mathcal{R}_k$, respectively. In particular, the first diagram on the rhs of Eq. (4.3) generates the metric-induced anomalous dimension A. Note that the sunset diagrams [like the second line of Eq. (4.2)] with the TT mode vanish due to its transverse property. We stress here that all modes in the metric fluctuations contribute to Z_ϕ, whereas the scalar potential receives corrections from only scalar modes. As a consequence the apparent gauge dependence may be eliminated by the redefinition of the Planck mass (3.19).

On the other hand, the use of the linear parametrization changes to the opposite situation:

$$\partial_t Z_\phi \sim \frac{d}{dp^2}\Big($$ 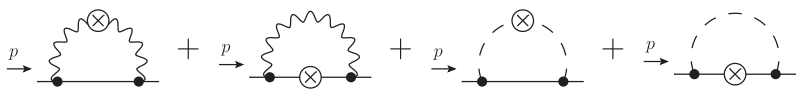 $$\Big)\Big|_{p^2=0},$$ (4.4)

$$\partial_t m_H^2 \sim -\tfrac{1}{2}$$ 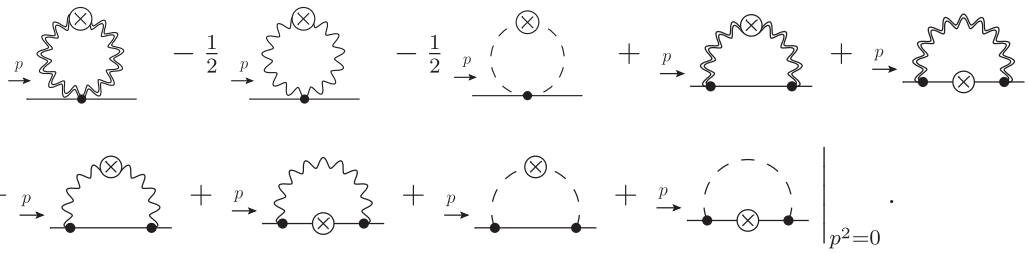 $$\Big|_{p^2=0}.$$ (4.5)

The first three tadpole diagrams on the rhs of Eq. (4.5) yield finite corrections to the metric-induced anomalous dimension A. An important fact is that the tadpole diagrams do not contribute to the flow equation of Z_ϕ in the linear parametrization.[2]

We thus expect that the exponential parametrization produces a larger value of η_ϕ and a smaller value of A than those in the linear parametrization case. Even though the exponential parametrization appears to be appropriate because the gauge dependence can be absorbed into the redefinition of the Planck mass, a larger value of η_ϕ may cause a potential problem in the present local potential approximation, which requires $\eta_\phi = 0$, and the derivative expansion for the effective action may not be valid. So let us first find the fixed points and critical exponents in our setup and compare the results with the linear parametrization [53], and then check how the anomalous dimensions A and η_ϕ affect the results. Eventually we would like to see if there is any optimal choice of β so as to make η_ϕ small.

[2]The diagrams with the spin-1 transverse mode is proportional to $\tilde{\alpha}$, so the Landau gauge $\tilde{\alpha} \to 0$ erases their contributions and then η_ϕ could be written as an apparent gauge invariant form, i.e., no β dependence, within contributions from scalar modes.

A. Fixed point

We first study how the fixed points for the Planck mass and the cosmological constant change in the exponential parametrization (1.2). To this end, we suppose hereafter that the Gaussian matter fixed point, namely, matter couplings, have only the trivial fixed point, $\tilde{m}_{H*}^2 = \tilde{\lambda}_* = 0$.

The fixed point of $\tilde{M}_P^2$ and $\tilde{V}$ in the linear parametrization with $\tilde{\alpha} = 0$, $\beta = 1$ is found to be [53]

$$\tilde{M}_{P*}^2 = 0.03366, \qquad \tilde{G}_{N*} = 1.182, \qquad \tilde{V}_* = 0.005420, \tag{4.6}$$

whereas in our exponential parametrization, we find

$$\tilde{M}_{P*}^2 = 0.03567, \quad \tilde{G}_{N*} = 1.1154, \quad \tilde{V}_* = 0.003539, \quad (\text{for } \tilde{\alpha} = 0, \beta = 1), \tag{4.7}$$

$$\tilde{M}_{P*}^2 = 0.020283, \quad \tilde{G}_{N*} = 1.9617, \quad \tilde{V}_* = 0.0025595, \quad (\text{for } \tilde{\alpha} = 0, \beta = -1), \tag{4.8}$$

$$\tilde{M}_{P*}^2 = 0.018998, \quad \tilde{G}_{N*} = 2.0944, \quad \tilde{V}_* = 0.0023747, \quad (\text{for } \tilde{\alpha} = 0, \beta = \infty). \tag{4.9}$$

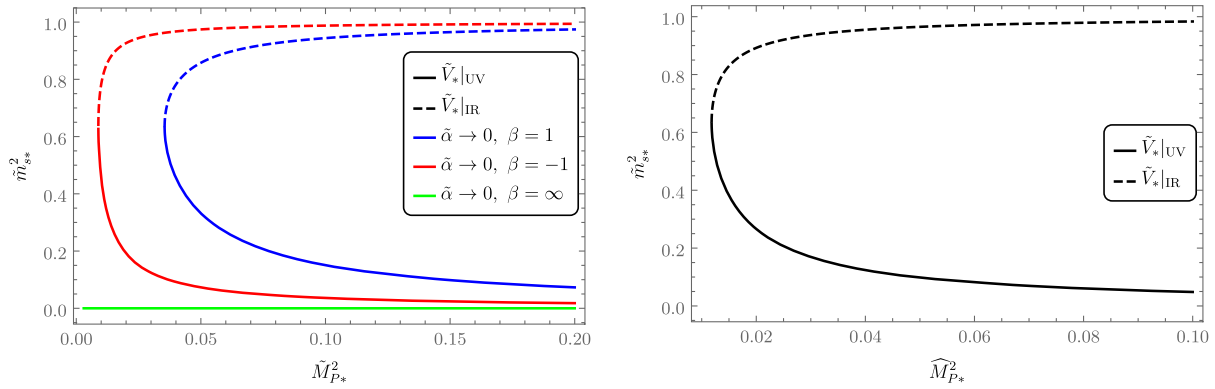

FIG. 2. The fixed-point value of the mass $\tilde{m}^2_{s*}$ as a function of the Planck mass squared. Left: $\tilde{m}^2_{s*}$ as a function of $\tilde{M}^2_{P*}$ with different gauge parameter choices. Right: $\tilde{m}^2_{s*}$ as a function of $\hat{M}^2_{P*}$. The solid and dashed lines show the $\tilde{m}^2_{s*}$ with $\tilde{V}_*|_{\rm UV}$ and $\tilde{V}_*|_{\rm IR}$ defined in Eq. (4.12), respectively.

In terms of the redefined Planck mass (3.19), one has, for $\tilde{\alpha}=0$, $\beta=1$

$$\hat{M}^2_{P*}=0.01189,\qquad \hat{G}_{N*}=3.3464,\qquad \tilde{V}_*=0.003539, \tag{4.10}$$

and for $\tilde{\alpha}=0$, $\beta=-1$,

$$\hat{M}^2_{P*}=0.027044,\quad \hat{G}_{N*}=1.4713,\quad \tilde{V}_*=0.0025595. \tag{4.11}$$

We do not find any reliable fixed point for $\tilde{\alpha}=0,\beta=\infty$, because the beta function is proportional to β. We will discuss this problem in detail in Sec. V. The fixed points (4.10) and (4.11) are related to (4.7) and (4.8), respectively, via the relation (3.19).

We next assume that a fixed point of the Planck mass exists and treat its fixed-point value as a constant parameter. Note that a small value of the Planck constant corresponds to a strong interaction of gravity.

With the redefinition (3.19), no dependence on the gauge parameter appears in the beta function of the cosmological constant since it does not have η_ϕ. For vanishing matter fixed points ($\tilde{m}^2_{H*}=\tilde{\lambda}_*=0$), we find from Eq. (3.13) fixed points of $\tilde{V}$:

$$\tilde{V}_*|_{\rm UV}=\frac{1+32\pi^2\hat{M}^2_{P*}-\sqrt{1-128\pi^2\hat{M}^2_{P*}+1024\pi^4\hat{M}^4_{P*}}}{128\pi^2},$$
$$\tilde{V}_*|_{\rm IR}=\frac{1+32\pi^2\hat{M}^2_{P*}+\sqrt{1-128\pi^2\hat{M}^2_{P*}+1024\pi^4\hat{M}^4_{P*}}}{128\pi^2}. \tag{4.12}$$

In Fig. 2, we plot $\tilde{m}^2_{s*}=2\tilde{V}_*(4(3-\tilde{\alpha})/(3-\beta)^2\tilde{M}^2_P)=2\tilde{V}_*/\hat{M}^2_{P*}$ instead of $\tilde{V}_*$. There also exist fixed points for smaller values of $\tilde{M}^2_{P*}$ or $\hat{M}^2_{P*}(\le\frac{2-\sqrt{3}}{32\pi^2}\simeq 0.00085)$; however, the fixed point values of $\tilde{m}^2_s$ there exceed 1 and thus we should exclude them. One can have these fixed points of $\tilde{V}$ written in terms of the original Planck mass $\tilde{M}^2_P$ by using Eq. (3.19).

We see from Fig. 2 that for larger values of $\hat{M}^2_{P*}$, the mass parameter $\tilde{m}^2_{s*}|_{\rm IR}$ converges to 1 which is a pole of the threshold functions $\ell^{2n}_p(-\tilde{m}^2_s)$ and then $\tilde{V}_*|_{\rm IR}$ corresponds to the IR fixed point, while $\tilde{V}_*|_{\rm UV}$ is the UV fixed point. In IR regimes, the flow of $\tilde{m}^2_s$ may come close to $\tilde{m}^2_*|_{\rm IR}$ which would induce large effects of the metric fluctuations on interactions including the cosmological constant itself. Since the metric fluctuations tend to make the cosmological constant smaller, it is argued in Refs. [99,100] that such an IR instability around a pole in the propagator could play a key role in realizing the tiny value of the cosmological constant.

B. Critical exponents

We evaluate the critical exponents for couplings in the scalar potential. Suppose here that the cosmological constant and the Planck mass have a nontrivial fixed point, while only the Gaussian fixed point is found for the scalar mass parameter and the quartic coupling.

The critical exponents are defined by

$$\theta_i=-\mathrm{eig}\left(\frac{\partial\beta_i}{\partial g_j}\right)\bigg|_{\tilde{g}=\tilde{g}_*}, \tag{4.13}$$

where $\tilde{g}_i=\{\tilde{M}^2_P,\tilde{V},\tilde{m}^2_H,\tilde{\lambda}\}$ and "eig" denotes evaluating eigenvalues of a matrix.

Taking only the diagonal parts in the stability matrix $\frac{\partial\beta_i}{\partial g_j}$ into account, the critical exponents of the cosmological constant, the scalar mass parameter, and the quartic coupling is approximately given, respectively, by

$$\theta_{\tilde{V}}\simeq-\frac{\partial\beta_{\tilde{V}}}{\partial\tilde{V}}\bigg|_{\tilde{g}=\tilde{g}_*}=4-A, \tag{4.14}$$

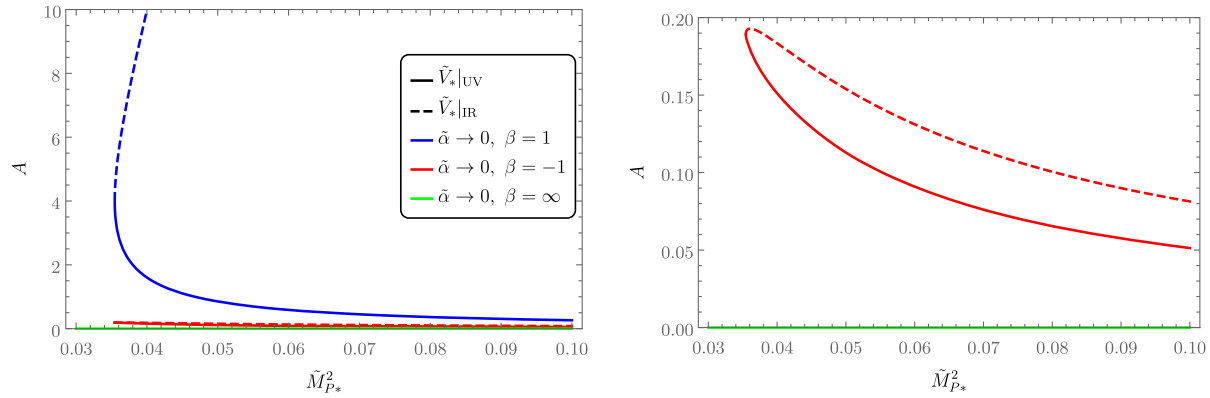

FIG. 3. The metric-induced anomalous dimension A as a function of $\tilde{M}_{P_*}$. The solid line corresponds to $V_*|_{\rm UV}$. For the fixed point of $\tilde{V}$, we use Eq. (4.12). The solid line corresponds to $V_*|_{\rm UV}$ and dashed line to $V_*|_{\rm IR}$. The rhs panel zooms in on the region of smaller A.

$$\theta_{\tilde{m}^2_H} \simeq -\left.\frac{\partial\beta_{\tilde{m}^2_H}}{\partial\tilde{m}^2_H}\right|_{\tilde{g}=\tilde{g}_*} = 2-\eta_\phi - A, \tag{4.15}$$

$$\theta_{\tilde{\lambda}} \simeq -\left.\frac{\partial\beta_\lambda}{\partial\tilde{\lambda}}\right|_{\tilde{g}=\tilde{g}_*} = -2\eta_\phi - A. \tag{4.16}$$

Note here that for the critical exponent of the beta function, one computes

$$\frac{\partial}{\partial\tilde{V}}\frac{1}{16\pi^2}\ell_0^4(-\tilde{m}_s^2)|_{\tilde{g}=\tilde{g}_*} = A. \tag{4.17}$$

In the case of the exponential parametrization, the TT spin-2 tensor does not couple to the scalar potential, so it does not induce the anomalous dimension A as can be seen in Eq. (3.16). The critical exponent of the cosmological constant evaluated by Eq. (4.14), however, may be insufficient because the mixing effects with the Planck mass cannot be neglected. More specifically, one should calculate

$$\theta_{\tilde{M}^2_P,\tilde{V}} = -{\rm eig}\left(\begin{array}{cc}\frac{\partial\beta_{\tilde{M}^2_P}}{\partial\tilde{M}^2_P} & \frac{\partial\beta_{\tilde{M}^2_P}}{\partial\tilde{V}}\\ \frac{\partial\beta_{\tilde{V}}}{\partial\tilde{M}^2_P} & \frac{\partial\beta_{\tilde{V}}}{\partial\tilde{V}}\end{array}\right)\Bigg|_{\substack{\tilde{M}^2_P=\tilde{M}^2_{P*}\\ \tilde{V}=\tilde{V}_*}}. \tag{4.18}$$

We plot the metric-induced anomalous dimension (3.16) as a function of $\tilde{M}^2_{P*}$ in Fig. 3 and as a function of $\hat{M}^2_{P*}$ in Fig. 4.

When η_ϕ can be neglected, the critical exponents of couplings in the scalar potential are given as a constant shift $-A$ from their canonical dimensions. In particular, the critical exponent of the scalar mass parameter becomes zero

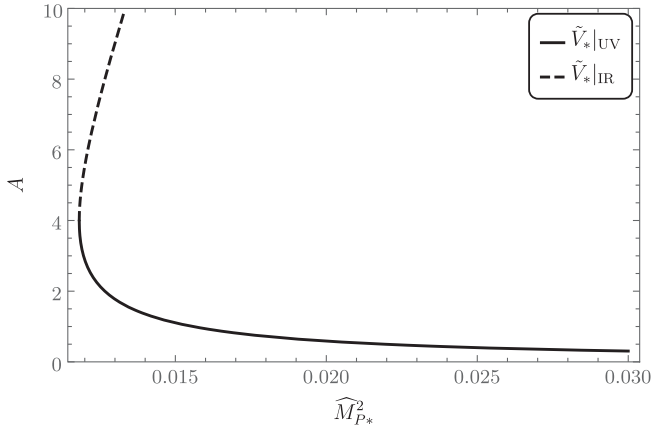

FIG. 4. The metric-induced anomalous dimension A as a function of $\hat{M}_{P_*}$. For the fixed point of $\tilde{V}$, we use Eq. (4.12).

(or, equivalently, $A=2$) at the fixed point value of the Planck mass,

$$\hat{M}^2_{P*} = \frac{1}{8\pi^2} \simeq 0.0126651. \tag{4.19}$$

The critical exponent of the cosmological constant vanishes when $A=4$ for which

$$\hat{M}^2_{P*} = \frac{2+\sqrt{3}}{32\pi^2} \simeq 0.0118167. \tag{4.20}$$

At this value, one has $\tilde{V}_*|_{\rm UV} = \tilde{V}_*|_{\rm IR}$.

Note here that using the linear parametrization produces the metric-induced anomalous dimension A given by

$$A|_{\rm linear} = \frac{1}{24\pi^2\tilde{M}^2_{P*}}\left[5\ell_1^2(-v_{0*}) + 3\tilde{\alpha}\ell_1^2(-\tilde{\alpha}v_{0*}) + \frac{2(3-\beta^2)}{(3-\beta)^2}\ell_1^2(-\tilde{m}^2_{L*}) + \left(4\tilde{\alpha}\frac{(3-\beta)^2+2(3-\beta^2)v_{0*}^2-4(3-\beta)^2v_{0*}}{(3-\beta)^4} + \frac{16\alpha^2v_{0*}^2}{(3-\beta)^4}\right)\ell_1^2(-\tilde{m}^2_{L*})\right], \tag{4.21}$$

where we have defined the mass of scalar modes in metric fluctuations:

$$\tilde{m}_L^2 = \frac{2(3-\beta^2)}{(3-\beta)^2} v_0 + \frac{4\tilde{\alpha}}{(3-\beta)^2}(1-v_0)v_0. \tag{4.22}$$

The first and second terms in Eq. (4.21) are contributions from the TT spin-2 tensor (i.e., graviton) and the transverse spin-1 vector, respectively, and the scalar modes of the metric fluctuations yield the remaining terms.

We now give numerical results for the critical exponents in the case of $\eta_\phi = 0$. At the fixed points of the original Planck mass squared $\tilde{M}_P^2$, the critical exponents are obtained for $\tilde{\alpha} \to 0$, $\beta = 1$ with Eq. (4.7) as

$$\theta_{1,2} = 2.59539 \pm 2.12893i, \qquad \theta_3 = -1.25264, \qquad \theta_4 = -3.25264, \tag{4.23}$$

for $\tilde{\alpha} \to 0$, $\beta \to -1$ with Eq. (4.8) as

$$\theta_1 = 3.6402, \qquad \theta_2 = 2.020, \qquad \theta_3 = 1.6437, \qquad \theta_4 = -0.35628, \tag{4.24}$$

and for $\tilde{\alpha} \to 0$, $\beta \to \infty$ with Eq. (4.9) as

$$\theta_1 = 4, \qquad \theta_2 = 2, \qquad \theta_3 = 2, \qquad \theta_4 = 0, \tag{4.25}$$

where θ_1 and θ_2 correspond to the critical exponents of the cosmological constant and the Planck mass squared, respectively, whereas θ_3 and θ_4 are those of the scalar mass parameter and the quartic coupling, respectively.

When the redefined Planck mass is used, we have found a fixed point for $\tilde{\alpha} \to 0$, $\beta = 1$ and $\tilde{\alpha} \to 0$, $\beta = -1$ as in Eqs. (4.10) and (4.11) at which the same critical exponents as Eqs. (4.23) and (4.24) are observed.

To understand these results, several comments are in order:

First, the negative critical exponents in Eq. (4.23) result from a large value of A and all scalar interactions including the scalar mass parameter become irrelevant. This is because the fixed point value (4.7) and $\tilde{\alpha} \to 0$, $\beta = 1$ yields $\tilde{m}_s^2 \simeq 0.59533$ which locates close to the pole of the threshold function. Indeed, for this value, one has $\ell_1^2(-\tilde{m}_s^2) \simeq 6.1071$. This casts a doubt to the validity of the result.

Second, the critical exponents for couplings of the scalar field for $\tilde{\alpha} \to 0$, $\beta \to \infty$ remain the same as the canonical ones (4.25). This comes from the fact that the β dependence appears in denominators of terms in the beta function of the scalar potential (3.7) in terms of the original Planck mass squared, so the limit $\beta \to \infty$ (and $\tilde{\alpha} \neq 3$) suppresses the metric fluctuations. This results in no metric-induced anomalous dimension even when the Planck mass has a finite fixed point value.

Third, if we use the redefined Planck mass squared, the beta function of the scalar potential has no explicit gauge-parameter dependence in contract to the case of the original Planck mass squared and the redefinition gives a finite A except for $\hat{M}_P^2 \to \infty$. In this case we get the same result as (4.24).

Finally, the discrepancy in $\beta \to \infty$ discussed above could be understood by taking η_ϕ into account. On the one hand, the metric fluctuation decouples from the scalar potential. On the other hand, the kinetic term of the scalar field gets a large contribution from the metric fluctuation, resulting in the anomalous dimension with the redefined Planck mass proportional to polynomials of β: $\eta_\phi \propto \frac{1}{\hat{M}_P^2} = \frac{(3-\beta)^2}{4(3-\tilde{\alpha})\tilde{M}_P^2}$. Thus, we expect that in the limit $\beta \to \infty$, the anomalous dimension η_ϕ diverges. Indeed, such a divergent behavior is observed in the linear parametrization case as well. This means that it is better that $|\beta|$ is not too large.

C. Effects of the anomalous dimension

Let us now discuss the effects of the anomalous dimension η_ϕ of the scalar field. In order for the derivative expansion to be valid for the effective action, $|\eta_\phi| < 1$ should be satisfied. We might allow somewhat larger $|\eta_\phi|$ within the current approximation because the loop effect of the scalar field on the Planck mass squared and the scalar potential has suppression factors such as $\eta_\phi/4$ and $\eta_\phi/6$; see Eqs. (3.7) and (3.20). In the linear parametrization, η_ϕ is of order 0.1 [53]. In particular, the choice $\beta = 1$ in the Landau gauge $\tilde{\alpha} \to 0$ gives the vanishing η_ϕ in the case of the linear parametrization. In the exponential parametrization, however, the TT mode, which is independent of the gauge parameters, may make a significant contribution to η_ϕ.

The rhs of Eq. (3.17) has the η_ϕ dependence arising from the scalar field propagator. Here, we consider two cases: (i) setting $\eta_\phi = 0$ in the rhs of Eq. (3.17); (ii) solving for η_ϕ in Eq. (3.17). We call the former (latter) "no-resummed" ("resummed") η_ϕ. The anomalous dimension η_ϕ as a function of $\tilde{M}_P^2$ is shown in Fig. 5 where we take $\tilde{\alpha} \to 0, \beta = -1$, and set $\tilde{V} = 0$ as an example. The resummed η_ϕ becomes relatively smaller than the no-resummed one. The larger the value of η_ϕ is, the larger is the difference between them. For a reasonable value of η_ϕ, however, we do not observe a large difference between (i) and (ii). In the analyses hereafter, we use the resummed η_ϕ.

Including η_ϕ, we obtain the fixed point values and the critical exponents for different gauge fixing values as follows:

(i) $\tilde{\alpha} \to 0$, $\beta = 1$

$$\tilde{M}^2_{P*} = 0.036381, \qquad \tilde{V}_* = 0.0036794, \qquad \eta_{\phi*} = -0.62968, \tag{4.26}$$

$$\theta_{1,2} = 2.40726 \pm 2.30995i, \qquad \theta_3 = -0.74809, \qquad \theta_4 = -2.1184, \tag{4.27}$$

(ii) $\tilde{\alpha} \to 0$, $\beta = -1$

$$\tilde{M}^2_{P*} = 0.020658, \qquad \tilde{V}_* = 0.0023414, \qquad \eta_{\phi*} = 1.4819, \tag{4.28}$$

$$\theta_1 = 3.7098, \qquad \theta_2 = 2.0541 \qquad \theta_3 = 0.1844, \qquad \theta_4 = -3.2975, \tag{4.29}$$

(iii) $\tilde{\alpha} \to 0$, $\beta \to \infty$

$$\tilde{M}^2_{P*} = 0.019837, \qquad \tilde{V}_* = 0.00195508, \qquad \eta_{\phi*} = 3.18076, \tag{4.30}$$

$$\theta_1 = 4, \qquad \theta_2 = 2.0795 \qquad \theta_3 = -1.1808, \qquad \theta_4 = -6.3615, \tag{4.31}$$

In terms of the redeifned Planck mass, we have
(i) $\tilde{\alpha} \to 0$, $\beta = 1$

$$\hat{M}^2_{P*} = 0.012127, \qquad \tilde{V}_* = 0.0036794, \qquad \eta_{\phi*} = 1.0067, \tag{4.32}$$

(ii) $\tilde{\alpha} \to 0$, $\beta = -1$

$$\hat{M}^2_{P*} = 0.027544, \qquad \tilde{V}_* = 0.0023414, \qquad \eta_{\phi*} = 1.0852, \tag{4.33}$$

for which we obtain the same critical exponents as the original Planck mass. The choice $\beta \to \infty$ does not yield the fixed point.

We find that the fixed point values are similar to the case with $\eta_\phi = 0$, while the critical exponents of the scalar mass parameter and the quartic coupling change. This is because an anomalous dimension of the scalar field of order 1 is induced. The beta functions for $\tilde{M}^2_P$ and $\tilde{V}$ have suppression factors, $\eta_\phi/4$ and $\eta_\phi/6$, as mentioned above, whereas the critical exponents of $\tilde{m}^2_H$ and $\tilde{\lambda}$ contains linear term in η_ϕ as given in Eqs. (4.15) and (4.16). In particular, the choice $\beta \to \infty$ for the original Planck mass yields $\eta_{\phi*} \approx 3$ which may be too large to accept the result. We study the gauge dependence of η_ϕ in the next section and investigate a suitable choice for the gauge parameters.

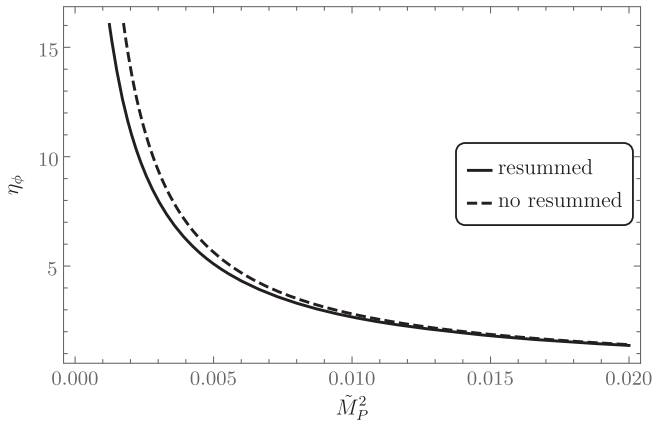

FIG. 5. The anomalous dimension of the scalar field η_ϕ as a function of $\tilde{M}^2_P$. We use $\tilde{\alpha} \to 0$, $\beta = -1$, and $\tilde{V} = 0$ for the presentation.

D. Anomalous dimensions as functions of the cosmological constant

Here we briefly examine how the critical exponents change as functions of the cosmological constant. In particular, it was observed in the previous section and in Ref. [53] that the critical exponent for the Higgs mass changes sign when $\tilde{V}_*$ approaches the pole of the propagator. This casts some doubt on the validity of this behavior. We have examined this and show the behavior of the metric-induced anomalous dimension A in Fig. 6. We plot A for the exponential parametrization and the linear one with $\tilde{\alpha} \to 0$, $\beta = 1$ for which $\tilde{m}^2_L = v_0$. We find that the metric-induced anomalous dimension in the linear parametrization takes a similar form to the case of the exponential parametrization:

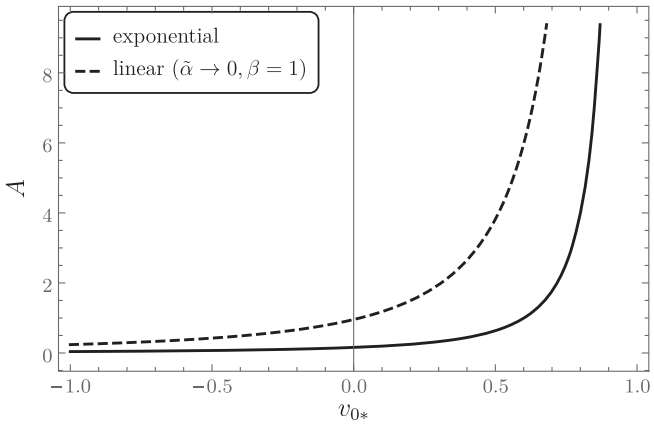

FIG. 6. The metric-induced anomalous dimension A defined in Eq. (3.16) at $\hat{M}^2_{P*} = 1/8\pi$ as functions of v_{0*} (solid line). The dashed line shows the Eq. (4.34) case where $\tilde{M}^2_{P*} = 1/8\pi$, the linear parametrization is used, and the gauge parameters are chosen as $\tilde{\alpha} = 0$, $\beta = 1$.

$$A|_{\text{linear}} = \frac{3}{8\pi^2 \tilde{M}^2_{P*}} \frac{1}{(1 - v_{0*})^2}. \tag{4.34}$$

For both linear and exponential parametrizations, there is a pole at $v_0 = 1$. In the linear parametrization, the TT mode in the metric fluctuations couples to the scalar potential and thus generates a finite contribution to A. Hence, $A|_{\text{linear}}$ tends to be larger than $A|_{\text{exp}}$.

This is opposite to the situation in the anomalous dimension of the scalar field. As discussed in the beginning of this section, the TT mode in the linear parametrization contributes to A, but not to η_ϕ. On the other hand, in the exponential parametrization, A does not receive the TT mode effects, whereas η_ϕ does.

V. GAUGE DEPENDENCE

Because some results depend on the choice of the gauge parameters, we would like to check quantitatively how the results change depending on the gauge parameters, and what physical implication may be extracted from the results even if they depend on the gauge. Here we examine this by changing the gauge parameters in the exponential parametrization. In terms of $\hat{M}^2_P$ defined in Eq. (3.19), the beta function of the cosmological constant has no apparent gauge dependence [see Eqs. (3.12) and (3.13)]. In this section, we concentrate on that of fixed point values of the Planck mass and the anomalous dimension of the scalar field η_ϕ.

A. Planck mass and cosmological constant

Let us look for fixed points of the Planck mass for various gauge parameters. To this end, we use the UV fixed point of the cosmological constant $\tilde{V}_*|_{\text{UV}}$ found in Eq. (4.12).

We first recall the singularities in gauge parameters. There is a singularity at $\beta = 3$. This singular behavior is observed in Refs. [45,90,91] and this is an artifact of our choice of gauge fixing function as discussed in Sec. II B. Besides, there is a singularity at $\tilde{\alpha} = 3$: The flow equation for the original Planck mass squared (3.20) has no singularity for any choice of $\tilde{\alpha}$, whereas the singularity at $\tilde{\alpha} = 3$ does not cancel in the beta function of the redefined one. This arises from the fact that the choice $\tilde{\alpha} = 3$ erases the propagator of the trace mode h, which is the only field in the metric fluctuations directly coupled to the scalar potential with the exponential parametrization. See Eq. (C5) in Appendix C and Eq. (D22) in Appendix D.

We show the gauge dependence of the fixed point value of the Planck mass squared $\tilde{M}^2_P$ and the cosmological constant $\tilde{\Lambda}$ in Fig. 7. Around the pole at $\beta = 3$, the fixed point values change drastically. For β well away from that pole, the fixed point values for any choice of $\tilde{\alpha}$ converge to the value $\tilde{M}^2_{P*} \approx 0.0190$ and $\tilde{\Lambda}_* \approx 0.125$ which are obtained by taking $\beta \to \pm\infty$. In the Landau gauge $\tilde{\alpha} \to 0$, such a convergence takes place faster.

In Fig. 8, we show the gauge dependence of the metric-induced anomalous dimension A which is proportional to $(3 - \tilde{\alpha})$. Therefore, A vanishes at $\tilde{\alpha} = 3$ and flips the overall sign. For $\tilde{\alpha} < 3$, the metric-induced anomalous dimension

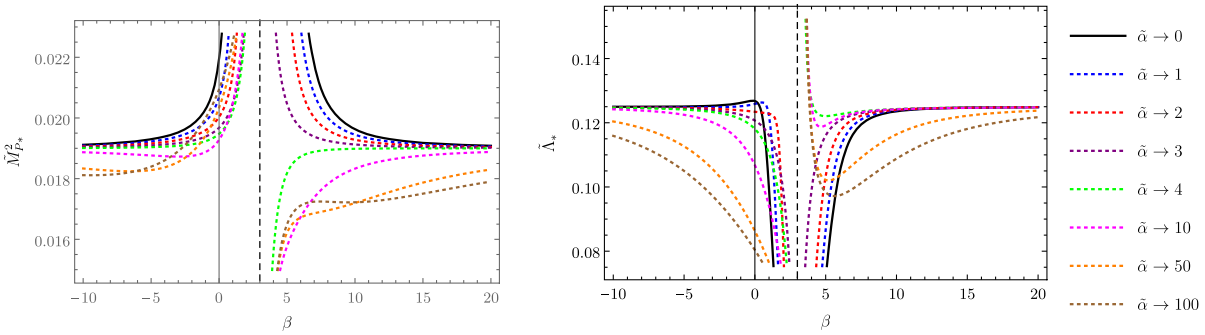

FIG. 7. Gauge dependence of the fixed point value of the Planck mass squared (left) the cosmological constant $\tilde{\Lambda}_* = \tilde{V}_*/\tilde{M}^2_{P*}$ (right). The vertical dashed line indicates the location of the pole at $\beta = 3$.

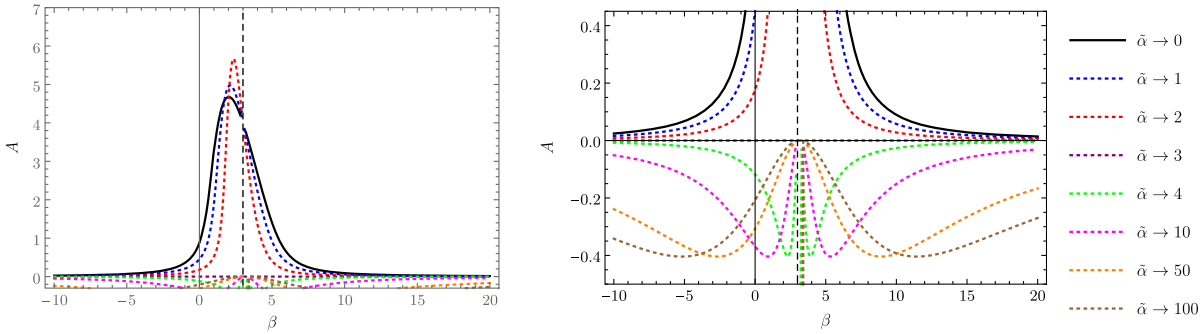

FIG. 8. Gauge dependence of the metric-induced anomalous dimension A with $\tilde{M}^2_{P*}$ and $\tilde{V}_*$. The rhs panel shows the region of smaller A in the lhs one. The vertical dashed line locates at the pole of $\beta = 3$.

exceeds 4 for $1 < \beta < 4$ and 2 for $0 < \beta < 5$, and these regions are not reliable.

Let us next check the redefined Planck mass. The gauge dependence of $\hat{M}^2_{P*}$ is depicted in Fig. 9. Here we have used the fixed point $\tilde{V}_*|_{\rm UV}$ given in Eq. (4.12) and therefore there is no reliable fixed point of $\tilde{V}$ for $\hat{M}^2_P \leq \frac{2+\sqrt{3}}{32\pi^2} \simeq 0.01182$. This region is shown by gray in Fig. 9. We see from this figure that $\hat{M}^2_P$ has a strong gauge dependence which is imported from the mass of scalar modes $\tilde{m}^2_s$. For $1 < \beta < 4$ in $\tilde{\alpha} < 3$, and for any β in $\tilde{\alpha} > 3$, the fixed point value of $\hat{M}^2_P$ is not found. Those just correspond to the region where A exceeds 4 or becomes negative. Thus, we should not take these gauge fixing parameters; the preferable region is $\tilde{\alpha} < 3$ and $\beta < 1$. Note that for $\beta \to \infty$, we have $\hat{M}^2_{P*}$ to be infinity. This is consistent with the fact that the metric fluctuation decouples from the scalar potential in the limit $\beta \to \infty$ as we have seen in the previous section. The gauge dependence of the metric-induced anomalous dimension is shown in Fig. 10. This is the same as in Fig. 8 except for $1 < \beta < 4$ in which A exceeds 4.

From the above analysis, we conclude that the region where the metric-induced anomalous dimension is larger than 4 should be excluded. This means that the cosmological constant cannot be irrelevant within the local potential approximation with $\eta_\phi = 0$.

Even if $A > 4$ is admitted, the cosmological constant cannot be irrelevant. To see this, we examine more precise behavior of the critical exponents of $\tilde{M}^2_P$ and $\tilde{V}$ given by the eigenvalues of the stability matrix (4.18):

$$\theta_{\tilde{M}^2_P,\tilde{V}} = -\frac{1}{2}\left\{\frac{\partial\beta_{\tilde{M}^2_P}}{\partial\tilde{M}^2_P} + \frac{\partial\beta_{\tilde{V}}}{\partial\tilde{V}} \pm \left(\frac{\partial\beta_{\tilde{M}^2_P}}{\partial\tilde{M}^2_P} - \frac{\partial\beta_{\tilde{V}}}{\partial\tilde{V}}\right)\sqrt{1 + \frac{4\frac{\partial\beta_{\tilde{V}}}{\partial\tilde{M}^2_P}\frac{\partial\beta_{\tilde{M}^2_P}}{\partial\tilde{V}}}{\left(\frac{\partial\beta_{\tilde{M}^2_P}}{\partial\tilde{M}^2_P} - \frac{\partial\beta_{\tilde{V}}}{\partial\tilde{V}}\right)^2}}\right\}\Bigg|_{\substack{\tilde{M}^2_P=\tilde{M}^2_{P*} \\ \tilde{V}=\tilde{V}_*}} . \tag{5.1}$$

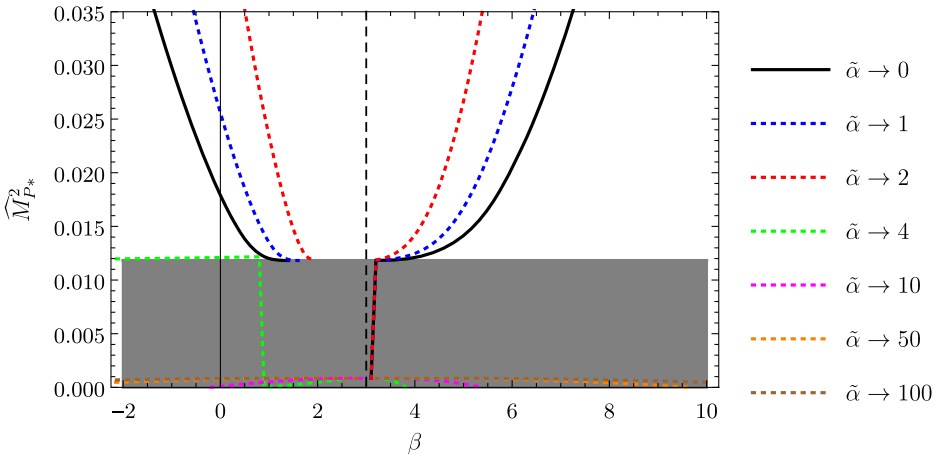

FIG. 9. Gauge dependence of the redefined Planck mass squared $\hat{M}^2_{P*}$. In the gray region, no UV fixed point value of $\tilde{V}$ is found. The vertical dashed line corresponds to the pole at $\beta = 3$.

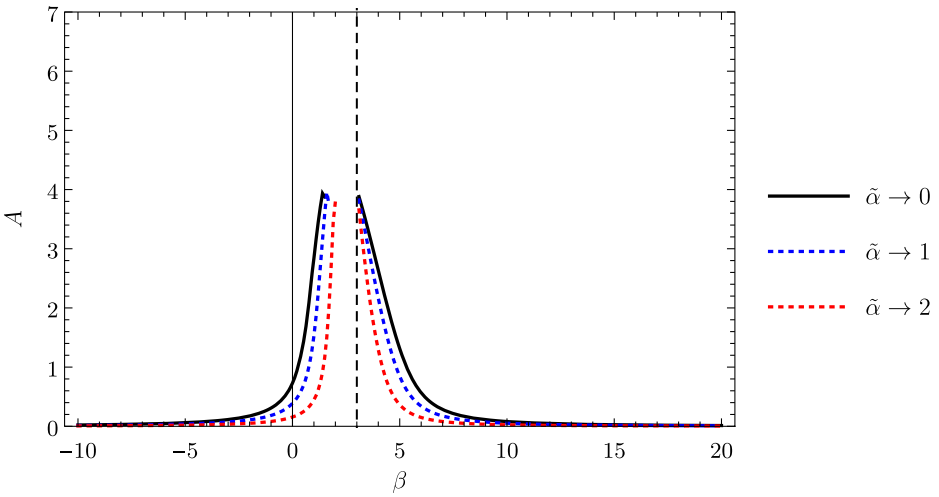

FIG. 10. Gauge dependence of the metric-induced anomalous dimension A with $\hat{M}^2_{P*}$ and $\tilde{V}_*|_{\rm UV}$. The pole at $\beta = 3$ is shown by the vertical dashed line.

When the off-diagonal parts are negligible, the critical exponents are simply given by the diagonal parts:

$$\theta_{\tilde{M}^2_P} \approx -\frac{\partial \beta_{\tilde{M}^2_P}}{\partial \tilde{M}^2_P}, \qquad \theta_{\tilde{V}} \approx -\frac{\partial \beta_{\tilde{V}}}{\partial \tilde{V}} = 4 - A. \tag{5.2}$$

On the other hand, when the off-diagonal parts are large so that inside of the square root in Eq. (5.1) becomes negative, the eigenvalues in Eq. (5.1) become imaginary and thus the real part of the critical exponents is commonly given by

$$\mathrm{Re}[\theta_{\tilde{M}^2_P,\tilde{V}}] \approx -\frac{1}{2}\left(\frac{\partial \beta_{\tilde{M}^2_P}}{\partial \tilde{M}^2_P} + \frac{\partial \beta_{\tilde{V}}}{\partial \tilde{V}}\right)\Bigg|_{\substack{\tilde{M}^2_P = \tilde{M}^2_{P*} \\ \tilde{V} = \tilde{V}_*}}, \tag{5.3}$$

for both $\tilde{M}^2_{P*}$ and $\tilde{V}_*$. This is what happens in Eq. (4.23).

In Fig. 11, we plot the β dependence of each element of the stability matrix in the Landau gauge $\tilde{\alpha} \to 0$. For β well away from the singularity at $\beta = 3$, the off-diagonal parts are negligibly small. In the region $0 < \beta < 6$, however, the off-diagonal part $\frac{\partial \beta_{\tilde{M}^2_P}}{\partial \tilde{V}}$ is significantly large, so that the critical exponents tend to be imaginary. Moreover, we see for $1 < \beta < 4$ that $-\frac{\partial \beta_{\tilde{V}}}{\partial \tilde{V}}$ turns to negative due to $A > 4$, while $-\frac{\partial \beta_{\tilde{M}^2_P}}{\partial \tilde{M}^2_P}$ is positive and large. Hence, the real part of the critical exponents (5.3) remains positive and the cosmological constant does not become irrelevant at least in the current setup. See Fig. 12 in which the β dependence of the real and imaginary parts of the critical exponents, $\theta_{\tilde{M}^2_P,\tilde{V}}$, are shown for the Landau gauge $\tilde{\alpha} \to 0$. One can see that the imaginary part appears for $0 < \beta < 6$.

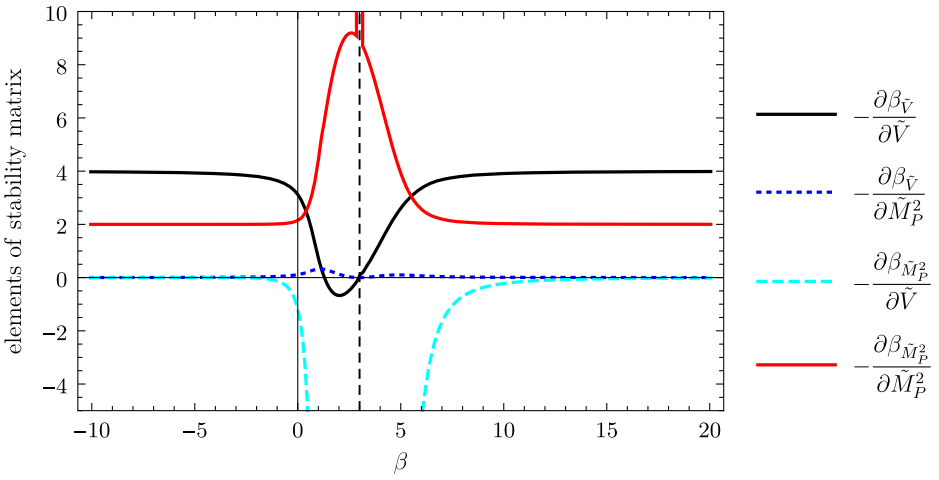

FIG. 11. Gauge dependence of each element of the stability matrix (4.18) in the Landau gauge $\tilde{\alpha} \to 0$. The position of the pole at $\beta = 3$ is shown by the vertical dashed line.

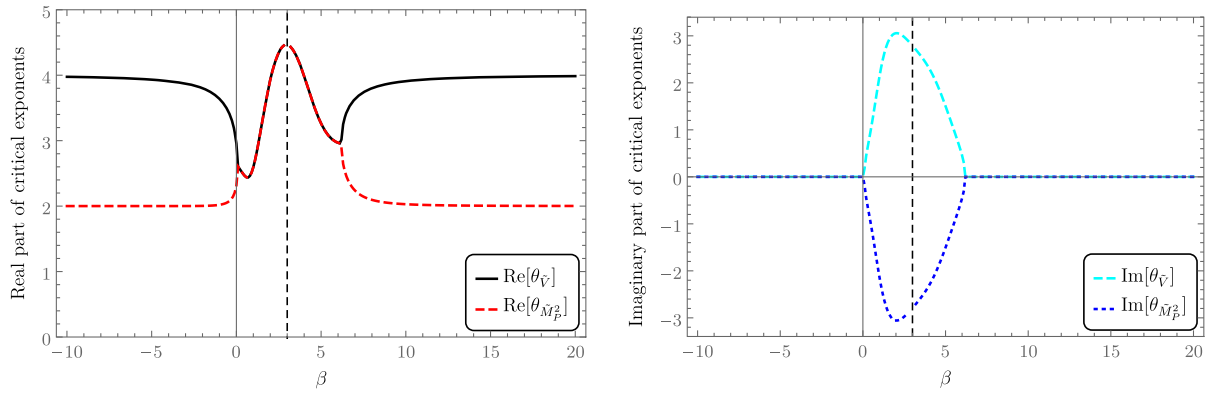

FIG. 12. Gauge dependence of the real (left) and imaginary (right) parts of the critical exponents $\theta_{\tilde{V}}$, $\theta_{\tilde{M}_P^2}$ in the Landau gauge $\tilde{\alpha} \to 0$. The vertical dashed line shows the location of the pole at $\beta = 3$.

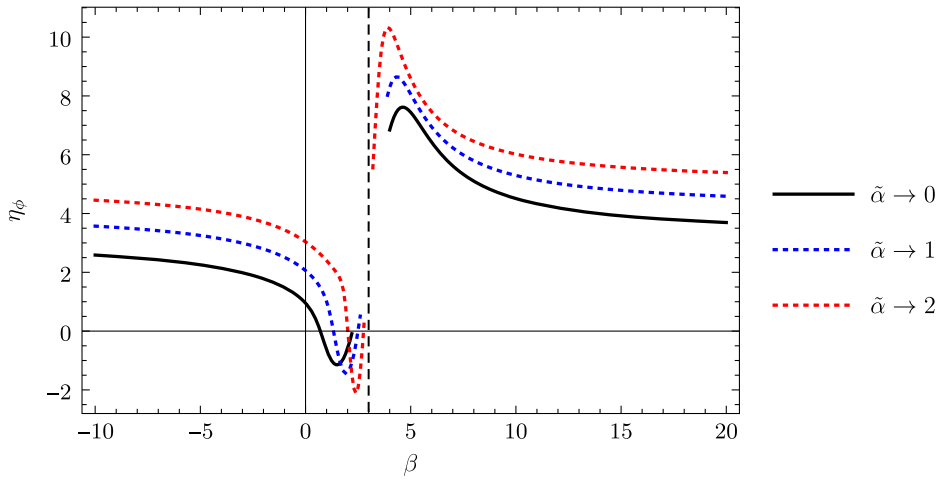

FIG. 13. Gauge dependence of η_ϕ. The vertical dashed line is located at $\beta = 3$.

Figures 11 and 12 also tell us that the choice around $0 < \beta < 6$ may not be appropriate in the sense of the principle of minimal sensibility. We thus conclude again that the values of β in this region which make $-\frac{\partial \beta_{\tilde{V}}}{\partial \tilde{V}} = 4 - A$ negative should be excluded if the redefined Planck mass is used.

B. Anomalous dimension of the scalar field

Here we study the gauge dependence of the anomalous dimension of the scalar field η_ϕ. Whereas we would have concluded that the gauge choice $0 < \beta < 5$ should be avoided, we have to pay attention to the magnitude of η_ϕ. A large value of η_ϕ violates the validity of the derivative expansion for the effective action of the scalar field. In particular, we expect that in the exponential parametrization, the tadpole diagram with a loop of the TT mode gives a significant contribution to η_ϕ. See Eq. (4.2). The explicit form of η_ϕ is given in Eq. (3.17). Indeed, in Sec. IV B, we have observed large values of η_ϕ for certain gauge parameter choices, e.g., $\eta_\phi \approx 3$ for $\beta \to \infty$ and $\tilde{\alpha} \to 0$.

We show the behavior of η_ϕ in (3.17) as a function of β for $\tilde{\alpha} = 0, 1, 2$ in Fig. 13. First, we see that η_ϕ takes larger values if $\beta > 3$ for any $\tilde{\alpha}$. This is not acceptable in terms of the validity of the derivative expansion. Second, although η_ϕ for $0 < \beta < 3$ is relatively smaller, it is sensitive to the variation in β. For $\beta < 0$ and $\tilde{\alpha} \neq 0$, one has $\eta_\phi \approx 3$ or larger which may be out of the validity of the derivative expansion. If we permit $\eta_\phi \approx 1$, the choice $-5 < \beta < 0$ with $\tilde{\alpha} = 0$ seems to be suitable together with the principle of minimal sensitivity.

VI. SUMMARY AND CONCLUSIONS

We have studied the parametrization and gauge dependences in the Higgs-gravity system by using the functional renormalization group. We have considered the Einstein-Hilbert truncation for a gravitational sector and used the exponential parametrization and compared the results in the linear parametrization. Assuming an Einstein spacetime for the background field, the beta functions for the Planck mass squared, the cosmological constant

and the scalar potential have been derived. We have used these results to study the parametrization and gauge dependences of the fixed points and the critical exponents. We find that the results do depend on these, but if we choose suitable range of gauge parameters, we may get reasonable and stable results under the change of gauge parameters, in accord with the principle of minimum sensitivity.

For the comparison of the parametrization dependence, the main features we have found are the following:

(1) An advantage of the exponential parametrization is that only the trace mode h in the metric fluctuations couples to the scalar potential including the cosmological constant. Consequently, the propagators of the other modes ($h^{TT}_{\mu\nu}$, ξ_μ and σ) in metric fluctuations have no artefactual poles arising from the cosmological constant.

(2) The gauge parameters appear in the scalar potential in a specific combination with the Planck mass, and thus the beta function of the scalar potential is written in an apparently gauge-independent form by the redefinition of the Planck mass (3.19). This allowed us to discuss the beta functions without gauge dependence.

(3) These advantages, however, are valid only if we can use the local potential approximation for the scalar field, i.e., $Z_\phi = 1$ (or, equivalently, $\eta_\phi = 0$). In the exponential parametrization, we have found that the loop corrections to η_ϕ come from all modes including the TT mode in the metric fluctuations which entail η_ϕ to be large. In the pure gravity, it appears that large $|\beta|$ is favored, but when the scalar fields exist, the gravity decouples from the scalar fields in the limit, and gives large contribution to the anomalous dimensions. Thus the exponential parametrization has also its limitation, and the linear parametrization may be better in this respect.

(4) These situations are opposite in the linear parametrization: the scalar potential receives loop effects of all modes in metric fluctuations, whereas only the spin-1 transverse vector and the scalar modes contribute to η_ϕ. Hence, although η_ϕ is small, the scalar potential have loop contributions from all modes which are strongly gauge dependent.

For the gauge dependence of the fixed points and critical exponents, we have shown

(1) There are singularities at $\beta = 3$ and $\tilde{\alpha} = 3$, and we should be well away from these singularities to get stable results. It appears that $\tilde{\alpha} < 3$ is preferable, and $\tilde{\alpha} = 0$ gives reasonable result. This point is also expected to be a fixed point if we let $\tilde{\alpha}$ run under the renormalization group.

(2) In the pure gravity, it appears that large $|\beta|$ is favored. When the scalar fields exist, the gravity decouples from the scalar fields in the limit, but gives large contribution to the anomalous dimensions. Considering the result on the gauge dependence of the anomalous dimensions, we find that $-5 \le \beta \le -1$ and $\tilde{\alpha} = 0$ gives reasonable results.

These investigations imply that the optimization in the gravitational sector tends to be in conflict with that in the Higgs sector. One needs to find a suitable choice for parameters such that both gravity and matter sectors are reasonably optimized. In our study, we have found that the region $\tilde{\alpha} \sim 0, -5 \le \beta \le -1$ seems to give optimized choice and the critical exponents are around

$$\theta_1 \sim 3.7, \quad \theta_2 \sim 2.1, \quad \theta_3 \sim 0.2, \quad \theta_4 \sim -3, \tag{6.1}$$

where η_ϕ gives relatively larger effect than A on the scalar mass parameter and the quartic coupling. Although the critical exponent of the Higgs mass parameter tends to be smaller than the canonical one, it still remains to be a relevant coupling within the present setups. We thus conclude that the critical exponent for the quartic coupling is negative, so that it is irrelevant, leading to the prediction to the low-energy physics, but other couplings are likely to be relevant. In particular we have shown that the cosmological constant never becomes irrelevant.

In general, it is expected that the improvement of truncation makes parameter dependence mild. For instance, it has been actually seen in Ref. [101] that by taking subleading effects into account, one can realize almost the gauge-parameter independence of the order parameter for spontaneous chiral symmetry breaking in quantum chromodynamics. An interesting question therefore is how much gauge dependence is reduced by the improvement of the gravitational sector, especially by constructing the full nonperturbative propagator [102–105]. It is also expected that systematic improvements of vertices [106–115] beyond the background-field approximation reduce gauge and parametrization dependences.

ACKNOWLEDGMENTS

We thank Roberto Percacci for valuable discussions. The work of N. O. was supported in part by the Grant-in-Aid for Scientific Research Fund of the JSPS (C) No. 16K05331, No. 20K03980, and Taiwan MOST 110-2811-M-008-510. The work of M. Y. is supported by the Alexander von Humboldt Foundation, the DFG Collaborative Research Centre "SFB 1225 (ISOQUANT)," and Germany's Excellence Strategy EXC-2181/1-390900948 (the Heidelberg Excellence Cluster STRUCTURES).

APPENDIX A: YORK DECOMPOSITION

The York decomposition is defined by

$$h_{\mu\nu} = h^{TT}_{\mu\nu} + \nabla_\mu \xi_\nu + \nabla_\nu \xi_\mu + \left(\nabla_\mu \nabla_\nu - \frac{1}{4}\bar{g}_{\mu\nu}\nabla^2\right)\sigma + \frac{1}{4}\bar{g}_{\mu\nu} h, \tag{A1}$$

where

$$\nabla^\mu h^{TT}_{\mu\nu} = \bar{g}^{\mu\nu} h^{TT}_{\mu\nu} = \nabla_\mu \xi^\mu = 0. \tag{A2}$$

When Eq. (A1) is squared, we get

$$\int d^4x\sqrt{\bar{g}}\left[h^{TT}_{\mu\nu}h^{TT\mu\nu} + 2\xi_\mu\left(\Delta_{L1} - \frac{1}{2}\bar{R}\right)\xi^\mu + \frac{3}{4}\sigma\Delta_{L0}\left(\Delta_{L0} - \frac{\bar{R}}{3}\right)\sigma + \frac{1}{4}h^2\right], \tag{A3}$$

where Δ_{Li} are Lichnerowicz Laplacians defined in Appendix B. Note that we can freely insert the covariant derivatives inside the above expression.

Let us here consider a Gaussian integral

$$1 = \int \mathcal{D}h_{\mu\nu} e^{-\int d^4x\sqrt{\bar{g}}h^{\mu\nu}h_{\mu\nu}}. \tag{A4}$$

Because of the York decomposition, this integral is rewritten as

$$1 = J\int \mathcal{D}h^{TT}_{\mu\nu}\mathcal{D}\xi_\mu\mathcal{D}\sigma\mathcal{D}h e^{-\int d^4x\sqrt{\bar{g}}[h^{TT}_{\mu\nu}h^{TT\mu\nu} + 2\xi_\mu(\Delta_{L1}-\frac{1}{2}\bar{R})\xi^\mu + \frac{3}{4}\sigma\Delta_{L0}(\Delta_{L0}-\frac{\bar{R}}{3})\sigma + \frac{1}{4}h^2]}, \tag{A5}$$

in which by performing the Gaussian integrals for each fields, the Jacobian should be identified with

$$J = \mathrm{Det}_{(1)}\left(\Delta_{L1} - \frac{\bar{R}}{2}\right)^{1/2}\mathrm{Det}_{(0)}\left[\Delta_{L0}\left(\Delta_{L0} - \frac{\bar{R}}{3}\right)\right]^{1/2} \equiv J_{\mathrm{grav1}}J_{\mathrm{grav0}}, \tag{A6}$$

where the suffices indicate which spin contributes. If we use new field variables

$$\hat{\xi}_\mu = \sqrt{\Delta_{L1} - \frac{\bar{R}}{2}}\xi_\mu; \qquad \hat{\sigma} = \sqrt{\Delta_{L0}}\sqrt{\Delta_{L0} - \frac{\bar{R}}{3}}\sigma, \tag{A7}$$

we do not have to introduce the Jacobian.

A similar decomposition should be made for the ghost fields, which is given in Eq. (2.9). Thanks to the inverse of the squared (Lichnerowicz) Laplacian in front of the scalar ghost C^L, the Jacobian associated to the decomposition does not arise.

APPENDIX B: LICHNEROWICZ LAPLACIANS

The Lichnerowicz Laplacians are defined as

$$\begin{aligned}
\Delta_{L2}T_{\mu\nu} &= -\nabla^2 T_{\mu\nu} + R_\mu{}^\rho T_{\rho\nu} + R_\nu{}^\rho T_{\mu\rho} - R_{\mu\rho\nu\sigma}T^{\rho\sigma} - R_{\mu\rho\nu\sigma}T^{\sigma\rho},\\
\Delta_{L1}V_\mu &= -\nabla^2 V_\mu + R_\mu{}^\rho V_\rho,\\
\Delta_{L0}S &= -\nabla^2 S.
\end{aligned} \tag{B1}$$

These operators have the useful properties of "commuting with covariant derivative" in the sense that

$$\begin{aligned}
\Delta_{L2}(\nabla_\mu\xi_\nu + \nabla_\nu\xi_\mu) &= \nabla_\mu\Delta_{L1}\xi_\nu + \nabla_\nu\Delta_{L1}\xi_\mu,\\
\Delta_{L2}(\nabla_\mu\nabla_\nu S) &= \nabla_\mu\nabla_\nu\Delta_{L0}S.
\end{aligned} \tag{B2}$$

APPENDIX C: VARIATIONS

We give variations for the effective action

$$\Gamma_k = \frac{Z_\phi}{2}\int d^4x\sqrt{g}g^{\mu\nu}\partial_\mu\phi\partial_\nu\phi + \int d^4x\sqrt{g}[U(\rho) - Z_N R]. \tag{C1}$$

With $\phi = \bar{\phi} + \varphi$ and the exponential parametrization (1.2), the second order of fluctuation fields in the effective action reads

$$\delta^2\Gamma_k = \frac{Z_\phi}{2}\int d^4x\sqrt{\bar{g}}[H_2^{\mu\nu}\partial_\mu\bar{\phi}\partial_\nu\bar{\phi} + H_1^{\mu\nu}\partial_\mu\varphi\partial_\nu\bar{\phi}] + \int d^4x\sqrt{\bar{g}}[V_1 - Z_N V_2], \tag{C2}$$

where

$$H_1^{\mu\nu} = h\bar{g}^{\mu\nu} - 2h^{\mu\nu}, \tag{C3}$$

$$H_2^{\mu\nu} = \frac{1}{8}h^2\bar{g}^{\mu\nu} + \frac{1}{2}h^\mu{}_\lambda h^{\nu\lambda} - \frac{1}{2}hh^{\mu\nu}, \tag{C4}$$

$$V_1 = \frac{1}{2}\left(\frac{h^2}{4}U(\bar{\rho}) + (U'(\bar{\rho}) + 2U''(\bar{\rho})\bar{\rho})\varphi^2 + U'(\bar{\rho})\sqrt{2\bar{\rho}}h\varphi\right), \tag{C5}$$

$$\begin{aligned} V_2 = {} & \frac{1}{4}h^2\bar{R} + h^{\mu\nu}\nabla_\mu\nabla_\nu h - 2h^{\mu\nu}\nabla_\nu\nabla_\alpha h_\mu{}^\alpha + h^{\mu\nu}\nabla^2 h_{\mu\nu} + \frac{3}{4}\nabla_\alpha h_{\mu\nu}\nabla^\alpha h^{\mu\nu} - \frac{1}{4}\nabla_\nu h\nabla^\nu h \\ & - \nabla_\mu h^{\mu\nu}\nabla_\alpha h_\nu{}^\alpha + \nabla^\nu h\nabla^\alpha h_{\nu\alpha} - \frac{1}{2}\nabla_\nu h_{\mu\alpha}\nabla^\alpha h^{\mu\nu} + \frac{1}{4}\nabla_\mu\nabla_\nu h^{\mu\alpha}h_\alpha{}^\nu - \frac{1}{4}\nabla^2 h^{\mu\alpha}h_{\alpha\mu} \\ & + h^{\mu\nu}h_{\alpha\beta}\bar{R}_{\mu\alpha\nu\beta} - \frac{1}{4}h^{\mu\alpha}h_\alpha{}^\nu\bar{R}_{\mu\nu} + h(\nabla_\mu\nabla_\nu h^{\mu\nu} - \nabla^2 h - h^{\mu\nu}\bar{R}_{\mu\nu}). \end{aligned} \tag{C6}$$

Note that in this work, we make the replacement $h_{\mu\nu} \to Z_N^{-1/2}h_{\mu\nu}$.

After employing the York decomposition, the Hessian has the following structure:

$$\Gamma_k^{(2)} = \frac{1}{2}\begin{pmatrix} (\Gamma_{h^{TT}h^{TT}})_{\mu\nu}{}^{\rho\sigma} & 0 & 0 & (\mathcal{V}_{h^{TT}h})_{\mu\nu} & (\mathcal{V}_{h^{TT}\varphi})_{\mu\nu} \\ 0 & (\Gamma_{\xi\xi})_\mu{}^\rho & 0 & 0 & (\mathcal{V}_{\xi\varphi})_\mu \\ 0 & 0 & \Gamma_{\sigma\sigma} & \Gamma_{\sigma h} & \Gamma_{\sigma\varphi} \\ (\mathcal{V}_{hh^{TT}})^{\rho\sigma} & 0 & \Gamma_{h\sigma} & \Gamma_{hh} & \Gamma_{h\varphi} \\ (\mathcal{V}_{\varphi h^{TT}})^{\rho\sigma} & (\mathcal{V}_{\varphi\xi})^\rho & \Gamma_{\varphi\sigma} & \Gamma_{\varphi h} & \Gamma_{\varphi\varphi} \end{pmatrix}, \tag{C7}$$

where each component is separated into the kinetic term and the vertex as

$$(\Gamma_{h^{TT}h^{TT}})_{\mu\nu}{}^{\rho\sigma} = (\mathcal{K}_{h^{TT}h^{TT}})(P_{TT})_{\mu\nu}{}^{\rho\sigma} + (\mathcal{V}_{h^{TT}h^{TT}})_{\mu\nu}{}^{\rho\sigma}, \tag{C8}$$

$$(\Gamma_{\xi\xi})_\mu{}^\rho = (\mathcal{K}_{\xi\xi})(P_1)_\mu{}^\rho + (\mathcal{V}_{\xi\xi})_\mu{}^\rho, \tag{C9}$$

$$\begin{pmatrix} \Gamma_{\sigma\sigma} & \Gamma_{\sigma h} & \Gamma_{\sigma\varphi} \\ \Gamma_{h\sigma} & \Gamma_{hh} & \Gamma_{h\varphi} \\ \Gamma_{\varphi\sigma} & \Gamma_{\varphi h} & \Gamma_{\varphi\varphi} \end{pmatrix} = \begin{pmatrix} \mathcal{K}_{\sigma\sigma} & \mathcal{K}_{\sigma h} & 0 \\ \mathcal{K}_{h\sigma} & \mathcal{K}_{hh} & 0 \\ 0 & 0 & \mathcal{K}_{\varphi\varphi} \end{pmatrix} + \begin{pmatrix} \mathcal{V}_{\sigma\sigma} & \mathcal{V}_{\sigma h} & \mathcal{V}_{\sigma\varphi} \\ \mathcal{V}_{h\sigma} & \mathcal{V}_{hh} & \mathcal{V}_{h\varphi} \\ \mathcal{V}_{\varphi\sigma} & \mathcal{V}_{\varphi h} & \mathcal{V}_{\varphi\varphi} \end{pmatrix}. \tag{C10}$$

Here, $(P_{TT})_{\mu\nu}{}^{\rho\sigma}$ is the transverse-traceless (TT) projector which is given in a flat spacetime background, where the Fourier transformation can be used, as

$$(P_{TT}(q))_{\mu\nu}{}^{\rho\sigma} = \frac{1}{2}[(P_1(q))_\mu{}^\rho (P_1(q))_\nu{}^\sigma + (P_1(q))_\mu{}^\sigma (P_1(q))_\nu{}^\rho] - \frac{1}{3}(P_1(q))_{\mu\nu}(P_1(q))^{\rho\sigma}, \tag{C11}$$

with the transverse vector projector

$$(P_1(q))_{\mu\nu} = \delta_{\mu\nu} - \frac{q_\mu q_\nu}{q^2}. \tag{C12}$$

The kinetic terms $\mathcal{K}$ are given in Eqs. (2.12), (2.13), and (2.15) without the $\bar{\phi}$ dependence. In particular, the kinetic term of the scalar modes is

$$\begin{pmatrix} \mathcal{K}_{\sigma\sigma} & \mathcal{K}_{\sigma h} & 0 \\ \mathcal{K}_{h\sigma} & \mathcal{K}_{hh} & 0 \\ 0 & 0 & \mathcal{K}_{\varphi\varphi} \end{pmatrix} = \begin{pmatrix} -\frac{3}{16}(\Delta_{L0})^2(\Delta_{L0} - \frac{\bar{R}}{3}) & -\frac{3}{16}\Delta_{L0}(\Delta_{L0} - \frac{\bar{R}}{3}) & 0 \\ -\frac{3}{16}\Delta_{L0}(\Delta_{L0} - \frac{\bar{R}}{3}) & -\frac{3}{16}(\Delta_{L0} + \frac{\bar{R}}{3}) + \frac{1}{4}\frac{V}{Z_N} & 0 \\ 0 & 0 & Z_\phi \Delta_{L0} + m^2 \end{pmatrix}$$
$$+ \frac{1}{\tilde{\alpha}} \begin{pmatrix} \frac{9}{16}\Delta_{L0}(\Delta_{L0} - \frac{\bar{R}}{3})^2 & \frac{3\beta}{16}\Delta_{L0}(\Delta_{L0} - \frac{\bar{R}}{3}) & 0 \\ \frac{3\beta}{16}\Delta_{L0}(\Delta_{L0} - \frac{\bar{R}}{3}) & \frac{\beta^2}{16}\Delta_{L0} & 0 \\ 0 & 0 & 0 \end{pmatrix}, \tag{C13}$$

while the vertices $\mathcal{V}$ arising from $H_1^{\mu\nu}$, $H_2^{\mu\nu}$, and V_1 have the $\bar{\phi}$ dependence.

APPENDIX D: FLOW GENERATORS

In this Appendix, we explicitly show contributions from each mode in the metric fluctuation. The regulator matrices $\mathcal{R}_k$ replace the Laplacians $z = \Delta_L$ in $\mathcal{K}$ to $P_k(z) = z + R_k(z)$. In this work, we employ the Litim cutoff function $R_k(z) = (k^2 - z)\theta(k^2 - z)$.

Denoting the regulated kinetic terms by $\tilde{\mathcal{K}}$, the flow equation is expanded into polynomials of $\mathcal{V}$ as

$$\begin{aligned} \partial_t \Gamma_k &= \frac{1}{2}\mathrm{Tr}[(\tilde{\mathcal{K}} + \mathcal{V})^{-1}\partial_t \mathcal{R}_k] \\ &= \frac{1}{2}\mathrm{Tr}[\tilde{\mathcal{K}}^{-1}\partial_t \mathcal{R}_k] - \frac{1}{2}\mathrm{Tr}[\tilde{\mathcal{K}}^{-1}\partial_t \mathcal{R}_k \tilde{\mathcal{K}}^{-1}\mathcal{V}] \\ &\quad + \mathrm{Tr}[\tilde{\mathcal{K}}^{-1}\partial_t \mathcal{R}_k \tilde{\mathcal{K}}^{-1}\mathcal{V}\tilde{\mathcal{K}}^{-1}\mathcal{V}] + \cdots. \end{aligned} \tag{D1}$$

Loop corrections to the cosmological constant and the Planck mass are involved in the first term in Eq. (D1), while those to the scalar potential $U(\rho)$ and the field renormalization factor Z_ϕ are obtained from the higher-order terms. The Hessians of the spin-2 TT and the spin-1 transverse vector modes have no dependence on the scalar potential U, so those does not induce quantum corrections to scalar-field interactions, while the spin-0 trace mode (h) has a U dependence in $\mathcal{K}_{hh}$ and the mixing terms ($\mathcal{V}_{h\varphi}$, $\mathcal{V}_{\varphi h}$) from which the scalar potential receives quantum corrections from the trace mode.

1. Heat kernel expansion

Before evaluating flow generators for each mode, we briefly summarize the heat kernel technique. The flow generator in this work typically takes a form

$$\zeta = \frac{1}{2}\mathrm{Tr}_{(i)} W[z = \Delta_i] = \frac{1}{2}\mathrm{Tr}_{(i)} \left.\frac{\partial_t (aR_k(z))}{(aP_k(z) + b)^{p+1}}\right|_{(\Phi)}, \tag{D2}$$

where a, b are scale-dependent constants and i denotes the internal space of a field Φ on which the Laplacian acts, e.g., $i = 2\mathrm{TT}$, 1T, etc. The heat kernel expansion gives

$$\zeta = \frac{1}{2(4\pi)^2}\int d^4x\sqrt{\bar{g}}[b_0^{(i)} Q_2[W] + b_2^{(i)} Q_1[W]\bar{R} + \cdots]. \tag{D3}$$

Here, $b_n^{(i)}$ are heat kernel coefficients and the threshold functions Q_n are defined by

$$Q_n[W] = \frac{1}{\Gamma(n)}\int_0^\infty dz\, z^{n-1} W[z], \quad (\text{for } n \geq 1), \tag{D4}$$

$$Q_{-n}[W] = (-1)^n \left.\frac{\partial^n W[z]}{\partial z^n}\right|_{z=0} \quad (\text{for } n \geq 0). \tag{D5}$$

When employing the optimized cutoff (3.3) for Eq. (D2), $Q_n[W]$ can be expressed in terms of the shorthand threshold function ℓ_p^{2n} introduced in Eq. (3.10) as

$$Q_n[W] = a^{-p}\left(1 - \frac{\eta_\Phi}{2(n+1)}\right)[2k^{2n-2p}\ell_p^{2n}(\tilde{m}_\Phi^2)], \tag{D6}$$

where we have defined $\eta_\Phi = -\partial_t a/a$ and $\tilde{m}_\Phi^2 = b/(k^2 a)$. For the heat kernel coefficients of the Lichnerowicz Laplacians, see, e.g., Ref. [91]. Note that in a flat spacetime, the variable z can be identified with loop momentum squared, q^2 so for $n \geq 1$

$$\frac{1}{2(4\pi)^2} Q_n[W] = \frac{1}{2}\int \frac{d^4q}{(2\pi)^4} \frac{q^{2n-4}}{\Gamma(n)} W[q^2]. \tag{D7}$$

2. Transverse-traceless spin-2 mode

The Hessian for the TT spin-2 mode is given in Eq. (2.12). Using the heat kernel expansion, one has

$$\begin{aligned}\pi^{\mathrm{TT}} &= \frac{1}{2}\mathrm{Tr}\frac{\partial_t \mathcal{R}_k}{\Gamma_k^{(2)} + \mathcal{R}_k}\bigg|_{h^{TT}h^{TT}} \\ &= \frac{1}{2}\mathrm{Tr}_{(2\mathrm{TT})}\left[\frac{\partial_t R_k}{P_k - \frac{\bar{R}}{2}}\right] \\ &= \frac{1}{(4\pi)^2}\int d^4x\sqrt{\bar{g}}\bigg[5\ell_0^4(0) \\ &\quad + k^2\left(-\frac{25}{6}\ell_0^2(0) + \frac{5}{2}\ell_0^4(0)\right)\bar{R}\bigg].\end{aligned} \tag{D8}$$

3. Spin-1 transverse vector modes

In the system, there are three spin-1 transverse vector modes, i.e., ξ_μ, C_μ^T ($\bar{C}_\mu^T$) and J_{grav1} which have the same structure of the Hessian as in Eqs. (2.10), (2.13), and (2.17). We denote these contributions by $\eta^{(1)}$, which is evaluated by the heat kernel technique:

$$\begin{aligned}\eta^{(1)} &= \frac{1}{2}\mathrm{Tr}\frac{\partial_t \mathcal{R}_k}{\Gamma_k^{(2)} + \mathcal{R}_k}\bigg|_{\xi\xi} - \mathrm{Tr}\frac{\partial_t \mathcal{R}_k}{\Gamma_k^{(2)} + \mathcal{R}_k}\bigg|_{\bar{C}^T C^T} \\ &\quad - \frac{1}{2}\mathrm{Tr}\frac{\partial_t \mathcal{R}_k}{\Gamma_k^{(2)} + \mathcal{R}_k}\bigg|_{J_{\mathrm{grav1}}} \\ &= -\frac{1}{2}\mathrm{Tr}_{(1\mathrm{T})}\left[\frac{\partial_t R_k}{P_k - \frac{\bar{R}}{2}}\right] \\ &= -\frac{1}{(4\pi)^2}\int d^4x\sqrt{\bar{g}}\bigg[3\ell_0^4(0) \\ &\quad + k^2\left(-\frac{1}{2}\ell_0^2(0) + \frac{3}{2}\ell_0^4(0)\right)\bar{R}\bigg].\end{aligned} \tag{D9}$$

4. Spin-0 scalar modes

We have (σ, h, ϕ), C^L ($\bar{C}^L$), and J_{grav0} as spin-0 scalar modes. Among them, two fields should be physical. One of physical modes is ϕ, while another is a linear combination of σ and h. Other modes are unphysical. Denoting $\pi^{(0)}$ and $\eta^{(0)}$ physical and unphysical modes, respectively, their flow generators are given by

$$\begin{aligned}\pi^{(0)} + \eta^{(0)} &= \frac{1}{2}\mathrm{Tr}\frac{\partial_t \mathcal{R}_k}{\Gamma_k^{(2)} + \mathcal{R}_k}\bigg|_{\mathrm{scalar}} - \mathrm{Tr}\frac{\partial_t \mathcal{R}_k}{\Gamma_k^{(2)} + \mathcal{R}_k}\bigg|_{\bar{C}^L C^L} \\ &\quad - \frac{1}{2}\mathrm{Tr}\frac{\partial_t \mathcal{R}_k}{\Gamma_k^{(2)} + \mathcal{R}_k}\bigg|_{J_{\mathrm{grav0}}}.\end{aligned} \tag{D10}$$

The last two terms can be simplified to be

$$\begin{aligned}&-\mathrm{Tr}\frac{\partial_t \mathcal{R}_k}{\Gamma_k^{(2)} + \mathcal{R}_k}\bigg|_{\bar{C}^L C^L} - \frac{1}{2}\mathrm{Tr}\frac{\partial_t \mathcal{R}_k}{\Gamma_k^{(2)} + \mathcal{R}_k}\bigg|_{J_{\mathrm{grav0}}} \\ &= -\mathrm{Tr}_{(0)}\left[\frac{\partial_t R_k}{P_k - \frac{\bar{R}}{3-\beta}}\right] - \frac{1}{2}\mathrm{Tr}_{(0)}\left[\frac{\partial_t R_k}{P_k - \frac{\bar{R}}{3}}\right] - \frac{1}{2}\mathrm{Tr}_{(0)}\left[\frac{\partial_t R_k}{P_k}\right] \\ &= -\frac{1}{(4\pi)^2}\int d^4x\sqrt{\bar{g}}\bigg[4\ell_0^4(0) \\ &\quad + k^2\left(\frac{2}{3}\ell_0^2(0) + \frac{9-\beta}{3(3-\beta)}\ell_0^4(0)\right)\bar{R}\bigg].\end{aligned} \tag{D11}$$

The first term on the rhs in Eq. (D10) is evaluated as follows: We first calculate the inverse matrix of the Hessian (2.15) with the regulator matrix $\mathcal{R}_k$ which replaces the Laplacians in the Hessian by P_k. Then, we evaluate the trace for the product of the inverse matrix of the Hessian and the regulator matrix differentiated by the scale, $\partial_t \mathcal{R}_k$. In this way, one obtains

$$\begin{aligned}\frac{1}{2}\mathrm{Tr}\frac{\partial_t \mathcal{R}_k}{\Gamma_k^{(2)} + \mathcal{R}_k}\bigg|_{\mathrm{scalar}} &= \frac{1}{(4\pi)^2}\int d^4x\sqrt{\bar{g}}\bigg[k^4 S_2(\tilde{\rho}) \\ &\quad + k^2\left(S_1(\tilde{\rho}) + \frac{1}{6}S_2(\tilde{\rho})\right)\bigg|_{\tilde{\rho}=0}\bar{R}\bigg],\end{aligned} \tag{D12}$$

where

$$\begin{aligned}S_2(\tilde{\rho}) &= 3\ell_0^4(0) + \ell_0^4(-\tilde{M}_s^2) \\ &\quad + 2\left(1 - \frac{\eta_\phi}{6}\right)\left[1 - 2\frac{4(3-\tilde{\alpha})}{(3-\beta)^2\tilde{M}_P^2}\tilde{U}(\tilde{\rho})\right] \\ &\quad \times \ell_0^4(-\tilde{M}_s^2(\tilde{\rho}))\ell_0^4(\tilde{M}_H^2(\tilde{\rho})),\end{aligned} \tag{D13}$$

$$\begin{aligned}S_1(\tilde{\rho}=0) &= \frac{6-\tilde{\alpha}}{6(3-\tilde{\alpha})} - \left[\frac{3-\tilde{\alpha}}{(3-\beta)^2} - \frac{1}{3-\beta} + \frac{1}{3-\tilde{\alpha}}\right] \\ &\quad \times \ell_1^2(-\tilde{m}_s^2).\end{aligned} \tag{D14}$$

5. Anomalous dimension of the scalar field

Let us derive the anomalous dimension of the scalar field, η_ϕ induced by the metric fluctuations. The full result is shown in Eq. (3.17).

We first note that we can consider a flat spacetime background $\bar{g}_{\mu\nu} = \delta_{\mu\nu}$ to obtain η_ϕ, so the Fourier transformation for fields can be employed, i.e.,

$$\frac{Z_\phi}{2}\int d^4x\delta^{\mu\nu}(\partial_\mu\phi)(\partial_\nu\phi)=\frac{Z_\phi}{2}\int\frac{d^4q}{(2\pi)^4}q^2\phi(q)\phi(-q). \tag{D15}$$

The flow equation for the renomalization factor of the scalar field is obtained by evaluating

$$\partial_t Z_\phi=\frac{1}{\Omega}\frac{d}{dp^2}\frac{\delta}{\delta\bar{\phi}(p)}\frac{\delta}{\delta\bar{\phi}(-p)}\partial_t\Gamma_k|_{p^2=0}, \tag{D16}$$

where $\Omega=\int d^4x=(2\pi)^4\delta^4(0)$ is a four-dimensional spacetime volume. Diagrammatically, there are the following contributions: From Eq. (D1),

$$\begin{aligned}\eta_\phi&=-\frac{1}{Z_\phi}\frac{1}{\Omega}\frac{d}{dp^2}\frac{\delta}{\delta\bar{\phi}(p)}\frac{\delta}{\delta\bar{\phi}(-p)}\left(-\frac{1}{2}\mathrm{Tr}\left[\tilde{\mathcal{K}}^{-1}\partial_t\mathcal{R}_k\tilde{\mathcal{K}}^{-1}\mathcal{V}\right]+\mathrm{Tr}\left[\tilde{\mathcal{K}}^{-1}\partial_t\mathcal{R}_k\tilde{\mathcal{K}}^{-1}\mathcal{V}\tilde{\mathcal{K}}^{-1}\mathcal{V}\right]\right)\Big|_{p^2=0}\\&=-\frac{1}{Z_\phi}\frac{1}{\Omega}\frac{d}{dp^2}\left(-\frac{1}{2}\right.\ \text{ 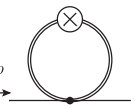 }\ +\ \text{ 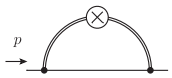 }\ +\ \text{ 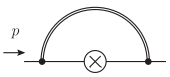 }\left.\right)\Big|_{p^2=0},\end{aligned} \tag{D17}$$

where solid and double-solid lines represent a scalar field and metric fluctuation fields $h_{\mu\nu}$, respectively, and the cross circle denotes the cutoff insertion in the propagator. For the first diagram (tadpole diagram), a vertex $H_2^{\mu\nu}$ given in Eq. (C4) contributes, whereas the second and third diagrams (sunset diagrams) have two vertices of $H_1^{\mu\nu}$. Below we calculate these contributions explicitly.

a. Tadpole diagram

Before computing contributions from the tadpole diagram, we consider the trace of $H_2^{\mu\nu}$, namely,

$$\delta_{\mu\nu}H_2^{\mu\nu}=\frac{1}{2}h_{\mu\nu}h^{\mu\nu}. \tag{D18}$$

Hence, due to the functional trace in the flow equation, the first and third terms in Eq. (C4) cancel each other, and thus only the second term in Eq. (C4) contributes. Moreover, as shown in Eq. (A3), the squared metric fluctuation field has no mixing term between different modes.

First, we evaluate the contribution from a TT-mode loop which is denoted by a double wiggly line below.

$$\begin{aligned}\eta_\phi\Big|^{\mathrm{2TT}}_{\mathrm{tadpole}}&=-\frac{1}{Z_\phi}\frac{1}{\Omega}\frac{d}{dp^2}\left(-\frac{1}{2}\ \text{ 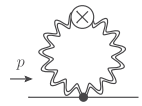 }\right)\Big|_{p^2=0}\\&=\frac{1}{Z_\phi}\frac{d}{dp^2}\frac{1}{\Omega}\frac{1}{2}\mathrm{Tr}\left[\tilde{\mathcal{K}}^{-1}\partial_t\mathcal{R}_k\tilde{\mathcal{K}}^{-1}(\mathcal{V})^{\mu\nu}{}_{\rho\sigma}(P_{TT})^{\rho\sigma}{}_{\mu\nu}\right]_{h^{TT}h^{TT}}\\&=\frac{1}{Z_\phi}\frac{d}{dp^2}\frac{1}{2}\mathrm{Tr}\left[\frac{\partial_t R_k(q)}{P_k(q)^2}\left(\frac{2Z_\phi}{Z_N}\delta^\nu_\sigma(p^\mu p_\rho)(P_{TT}(q))^{\rho\sigma}{}_{\mu\nu}\right)\right]\\&=\frac{5}{2Z_N}\frac{1}{2}\int\frac{d^4q}{(2\pi)^4}\frac{\partial_t R_k(q)}{P_k(q)^2}=\frac{5}{(4\pi)^2}\frac{1}{\tilde{M}_P^2}\ell_1^4(0),\end{aligned} \tag{D19}$$

where $(P_{TT}(q))^{\rho\sigma}{}_{\mu\nu}$ is defined in Eq. (C11).

Second, the loop effect of the transverse spin-1 mode is calculated. Denoting it by a single wiggly line, we obtain

$$\begin{aligned}\eta_\phi\Big|^{\rm 1T}_{\rm tadpole} &= -\frac{1}{Z_\phi}\frac{1}{\Omega}\frac{d}{dp^2}\left(-\frac{1}{2}\right)\Big|_{p^2=0} \\ &= \frac{1}{Z_\phi}\frac{d}{dp^2}\frac{1}{\Omega}\frac{1}{2}{\rm Tr}\left[\tilde{\mathcal{K}}^{-1}\partial_t\mathcal{R}_k\tilde{\mathcal{K}}^{-1}(\mathcal{V})^\mu{}_\nu(P_1)^\nu{}_\mu\right]_{\xi\xi} \\ &= \frac{1}{Z_\phi}\frac{d}{dp^2}\frac{1}{2}{\rm Tr}\left[\frac{2P_k\partial_t R_k(q)}{P_k(q)^4}\left(\frac{\tilde{\alpha}Z_\phi}{Z_N}q^2\left\{\frac{1}{4}\delta^{\mu\nu}\delta^{\alpha\beta}+\delta^{\alpha\mu}\delta^{\beta\nu}\right\}(P_1(q))_{\alpha\beta}p_\mu p_\nu\right)\right] \\ &= \frac{3\tilde{\alpha}}{2Z_N}\int\frac{d^4q}{(2\pi)^4}q^2\frac{\partial_t R_k(q)}{P_k(q)^3} = \frac{12\tilde{\alpha}}{(4\pi)^2}\frac{1}{\tilde{M}_P^2}\ell_2^6(0).\end{aligned} \tag{D20}$$

Note that we have redefined the transverse vector mode as $\xi_\mu \to \tilde{\alpha}^{1/2}\xi_\mu$.

Finally, let us calculate contributions from the scalar modes in the metric fluctuations for which we need the 2×2 vertex matrix,

$$\begin{pmatrix}\mathcal{V}_{\sigma\sigma} & \mathcal{V}_{\sigma h}\\ \mathcal{V}_{h\sigma} & \mathcal{V}_{hh}\end{pmatrix}. \tag{D21}$$

Their propagators are given as a 2×2 matrix, i.e., the regulated propagator matrix reads

$$\tilde{\mathcal{K}}^{-1}|_{2\times 2} = \frac{16}{P_k - k^2\tilde{m}_s^2}\begin{pmatrix}-\frac{1}{3P_k^2}\frac{(\beta^2-3\tilde{\alpha})P_k+4\tilde{\alpha}k^2v_0}{(\beta-3)^2P_k} & \frac{(\beta-\tilde{\alpha})}{(\beta-3)^2P_k}\\ \frac{(\beta-\tilde{\alpha})}{(\beta-3)^2P_k} & \frac{(\tilde{\alpha}-3)}{(\beta-3)^2}\end{pmatrix}, \tag{D22}$$

with $\tilde{m}_s^2 = \frac{4(3-\tilde{\alpha})}{(3-\beta)^2}v_0$ and the regulator matrix

$$\mathcal{R}_k|_{2\times 2} = \frac{1}{16}\begin{pmatrix}\frac{3(3-\tilde{\alpha})}{\tilde{\alpha}}(P_k^3-q^6) & \frac{3(\beta-\tilde{\alpha})}{\alpha}(P_k^2-q^4)\\ \frac{3(\beta-\tilde{\alpha})}{\tilde{\alpha}}(P_k^2-q^4) & \frac{\beta^2-3\tilde{\alpha}}{\tilde{\alpha}}(P_k-q^2)\end{pmatrix}. \tag{D23}$$

As mentioned above, the traced $H_2^{\mu\nu}$ contains no mixing vertex between σ and h, so we define the vertex matrix of scalar modes as the following diagonal form

$$\begin{pmatrix}\mathcal{V}_{\sigma\sigma} & \mathcal{V}_{\sigma h}\\ \mathcal{V}_{h\sigma} & \mathcal{V}_{hh}\end{pmatrix} \to \mathcal{V}|_{2\times 2} = \frac{Z_\phi}{Z_N}\Omega\frac{p^2}{16}\begin{pmatrix}3q^4 & 0\\ 0 & 1\end{pmatrix}, \tag{D24}$$

where we already performed the symmetrization for the loop momenta; $q^\mu q^\nu \to \frac{q^2}{4}\delta^{\mu\nu}$ and p_μ are external momenta.

We denote the propagator of scalar modes in the metric fluctuations by a dashed line and evaluate contributions from their tadpole diagram as follows:

$$\begin{aligned}\eta_\phi\Big|^{\rm scalar}_{\rm tadpole} &= -\frac{1}{Z_\phi}\frac{1}{\Omega}\frac{d}{dp^2}\left(-\frac{1}{2}\right)\Big|_{p^2=0} \\ &= \frac{1}{Z_\phi}\frac{1}{\Omega}\frac{d}{dp^2}\frac{1}{2}{\rm Tr}\left[\tilde{\mathcal{K}}^{-1}\partial_t\mathcal{R}_k\tilde{\mathcal{K}}^{-1}\mathcal{V}\right]_{2\times 2} \\ &= -\frac{1}{(4\pi)^2}\frac{4(3-\tilde{\alpha})}{(3-\beta)^2\tilde{M}_P^2}\left[\frac{1}{4}\ell_1^2(-\tilde{m}_s^2) - \frac{9\tilde{\alpha}(3-\beta)^2}{(3-\tilde{\alpha})^2}\ell_0^8(0)\right. \\ &\quad \left. + \frac{9(\tilde{\alpha}-\beta)^2}{(3-\tilde{\alpha})^2}\left(\ell_1^6(-\tilde{m}_s^2)+2\ell_0^8(-\tilde{m}_s^2)\right)\right].\end{aligned} \tag{D25}$$

To summarize, the total contributions from the tadpole diagrams are the sum of Eqs. (D19), (D20), and (D25).

Here we briefly comment on the case of the linear parametrization for which the vertex with two-metric fluctuations reads

$$H_2^{\mu\nu} = \left(-\frac{1}{4}h^{\alpha\beta}h_{\alpha\beta} + \frac{1}{8}h^2\right)\bar{g}^{\mu\nu} + h^\mu{}_\lambda h^{\nu\lambda} - \frac{1}{2}hh^{\mu\nu}. \tag{D26}$$

Taking the trace for this, we find that $\bar{g}_{\mu\nu}H_2^{\mu\nu} = 0$, thus there are no contributions from the tadpole diagrams in the linear parametrization.

b. Sunset diagrams

We compute the anomalous dimension of the scalar field from the sunset diagrams which are given by last two terms in Eq. (D17). We note that although the three-point vertex $\bar{\phi} - h - \varphi$ arises from the scalar mass term $m^2\sqrt{g}\phi^2$, we do not take it into account by assuming that scalar interactions have only the Gaussian fixed point. Thus, we consider contributions from only $H_1^{\mu\nu}$.

We first recognize that the sunset diagrams with the TT mode propagator does not contribute because within the flow generator, loop momenta q^μ included in the vertex $\mathcal{V}_{h^{TT}\varphi}$ contract with the TT projector (C11) and give $q^\mu(P_{TT}(q))^{\rho\sigma}{}_{\mu\nu} = 0$.

We next consider the anomalous dimension η_ϕ induced by the interactions $\mathcal{V}_{\xi\varphi}$ and $\mathcal{V}_{\varphi\xi}$. The flow equation contains the following algebraic computation:

$$\mathrm{Tr}[(iq^\rho\delta^\sigma_\alpha)q_\rho p_\sigma (iq^\mu\delta^\nu_\beta)q_\mu p_\nu (P_1(q))^{\alpha\beta}] = -\frac{3}{4}q^2p^2. \tag{D27}$$

Using this, we obtain

$$\begin{aligned}
\eta_\phi\Big|^{1\mathrm{T}}_{\mathrm{sunset}} &= -\frac{1}{Z_\phi}\frac{1}{\Omega}\frac{d}{dp^2}\left(\quad + \quad\right)\Big|_{p^2=0} \\
&= -\frac{1}{Z_\phi}\frac{1}{\Omega}\frac{d}{dp^2}\mathrm{Tr}\left[\tilde{\mathcal{K}}^{-1}\partial_t\mathcal{R}_k\tilde{\mathcal{K}}^{-1}\mathcal{V}\tilde{\mathcal{K}}^{-1}\mathcal{V}\right]_{\xi\varphi} \\
&= \frac{3}{4}\frac{\tilde{\alpha}}{Z_N}\mathrm{Tr}\left[\frac{Z_\phi}{Z_\phi P_k(q)+m^2}\frac{q^2\partial_t R_k(q)}{P_k(q)^2}\right] + \frac{3}{4}\frac{\tilde{\alpha}}{Z_N}\mathrm{Tr}\left[\frac{Z_\phi q^2\partial_t(Z_\phi R_k(q))}{(Z_\phi P_k(q)+m^2)^2}\frac{1}{P_k(q)}\right] \\
&= \tilde{\alpha}\frac{1}{Z_N}\frac{3}{4}\int\frac{d^4q}{(2\pi)^4}\frac{q^2\partial_t R_k}{P_k^2}\frac{1}{P_k+\tilde{m}_H^2k^2} + \tilde{\alpha}\frac{1}{Z_N}\frac{3}{4}\int\frac{d^4q}{(2\pi)^4}\frac{q^2\partial_t(Z_\phi R_k)/Z_\phi}{(P_k+\tilde{m}_H^2k^2)^2}\frac{1}{P_k} \\
&= \tilde{\alpha}\frac{6}{(4\pi)^2}\frac{1}{\tilde{M}_P^2}\left[\ell_1^6(0)\ell_0^2(\tilde{m}_H^2) + \left(1-\tfrac{\eta_\phi}{6}\right)\ell_1^6(\tilde{m}_H^2)\ell_0^2(0)\right],
\end{aligned} \tag{D28}$$

where we have used $q^\mu(P_1(q))_{\mu\nu} = 0$ and $p_\beta(P_1)^{\beta\alpha}p_\alpha = 3p^2/4$.

Next, we evaluate loop effects of spin-0 modes for which the following 3×3 vertex matrix is needed:

$$\begin{pmatrix} 0 & 0 & \mathcal{V}_{\sigma\varphi} \\ 0 & 0 & \mathcal{V}_{h\varphi} \\ \mathcal{V}_{\varphi\sigma} & \mathcal{V}_{\varphi h} & 0 \end{pmatrix}. \tag{D29}$$

The flow equation for the two-point function of $\bar{\phi}$ is given by

$$
\begin{aligned}
&\frac{\delta^2(\partial_t\Gamma_k)}{\delta\bar{\phi}(p)\delta\bar{\phi}(-p)} \\
&= \frac{\delta^2}{\delta\bar{\phi}(p)\delta\bar{\phi}(-p)}\mathrm{Tr}\left[\begin{pmatrix} 0 & 0 & \mathcal{V}_{\sigma\varphi} \\ 0 & 0 & \mathcal{V}_{h\varphi} \\ \mathcal{V}_{\varphi\sigma} & \mathcal{V}_{\varphi h} & 0 \end{pmatrix}\begin{pmatrix} \tilde{\mathcal{K}}_{\sigma\sigma} & \tilde{\mathcal{K}}_{\sigma h} & 0 \\ \tilde{\mathcal{K}}_{\sigma h} & \tilde{\mathcal{K}}_{hh} & 0 \\ 0 & 0 & \tilde{\mathcal{K}}_{\varphi\varphi} \end{pmatrix}^{-1}\begin{pmatrix} \partial_t R_{\sigma\sigma} & \partial_t R_{\sigma h} & 0 \\ \partial_t R_{\sigma h} & \partial_t R_{hh} & 0 \\ 0 & 0 & \partial_t R_{\varphi\varphi} \end{pmatrix}\right. \\
&\quad\left.\times\begin{pmatrix} \tilde{\mathcal{K}}_{\sigma\sigma} & \tilde{\mathcal{K}}_{\sigma h} & 0 \\ \tilde{\mathcal{K}}_{\sigma h} & \tilde{\mathcal{K}}_{hh} & 0 \\ 0 & 0 & \tilde{\mathcal{K}}_{\varphi\varphi} \end{pmatrix}^{-1}\begin{pmatrix} 0 & 0 & \mathcal{V}_{\sigma\varphi} \\ 0 & 0 & \mathcal{V}_{h\varphi} \\ \mathcal{V}_{\varphi\sigma} & \mathcal{V}_{\varphi h} & 0 \end{pmatrix}\begin{pmatrix} \tilde{\mathcal{K}}_{\sigma\sigma} & \tilde{\mathcal{K}}_{\sigma h} & 0 \\ \tilde{\mathcal{K}}_{\sigma h} & \tilde{\mathcal{K}}_{hh} & 0 \\ 0 & 0 & \tilde{\mathcal{K}}_{\varphi\varphi} \end{pmatrix}^{-1}\right] \\
&= \frac{\delta^2}{\delta\bar{\phi}(p)\delta\bar{\phi}(-p)}\mathrm{Tr}\left[\frac{1}{\tilde{\mathcal{K}}_{\varphi\varphi}}\begin{pmatrix} \mathcal{V}_{\sigma\varphi}\mathcal{V}_{\varphi\sigma} & \mathcal{V}_{\sigma\varphi}\mathcal{V}_{\varphi h} \\ \mathcal{V}_{h\varphi}\mathcal{V}_{\varphi\sigma} & \mathcal{V}_{h\varphi}\mathcal{V}_{\varphi h} \end{pmatrix}\left[\tilde{\mathcal{K}}^{-1}\partial_t\mathcal{R}_k\tilde{\mathcal{K}}^{-1}\right]_{2\times 2}\right] \\
&\quad + \frac{\delta^2}{\delta\bar{\phi}(p)\delta\bar{\phi}(-p)}\mathrm{Tr}\left[\frac{\partial_t R_{\varphi\varphi}}{\tilde{\mathcal{K}}_{\varphi\varphi}^2}\begin{pmatrix} \mathcal{V}_{\sigma\varphi}\mathcal{V}_{\varphi\sigma} & \mathcal{V}_{\sigma\varphi}\mathcal{V}_{\varphi h} \\ \mathcal{V}_{h\varphi}\mathcal{V}_{\varphi\sigma} & \mathcal{V}_{h\varphi}\mathcal{V}_{\varphi h} \end{pmatrix}\tilde{\mathcal{K}}^{-1}\Big|_{2\times 2}\right] \\
&= \quad p \rightarrow \quad + \quad p \rightarrow \quad .
\end{aligned}
\tag{D30}
$$

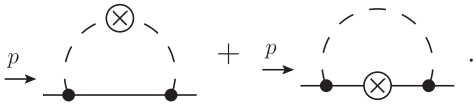

Here, $\tilde{\mathcal{K}}^{-1}|_{2\times 2}$ and $\mathcal{R}_k|_{2\times 2}$ are defined in Eqs. (D22) and (D23), respectively, and the vertex matrix is reduced to the 2×2 matrix

$$
\begin{aligned}
&\frac{\delta^2}{\delta\bar{\phi}(p)\delta\bar{\phi}(-p)}\begin{pmatrix} \mathcal{V}_{\sigma\varphi}\mathcal{V}_{\varphi\sigma} & \mathcal{V}_{\sigma\varphi}\mathcal{V}_{\varphi h} \\ \mathcal{V}_{\sigma\varphi}\mathcal{V}_{\varphi h} & \mathcal{V}_{h\varphi}\mathcal{V}_{\varphi h} \end{pmatrix} \\
&= \Omega\frac{Z_\phi^2}{M_P^2}\begin{pmatrix} 2(q^\mu q^\nu - \frac{\delta^{\mu\nu}}{4}q^2)q_\mu p_\nu \times 2(q^\rho q^\sigma - \frac{\delta^{\rho\sigma}}{4}q^2)q_\rho p_\sigma & 2(q^\mu q^\nu - \frac{\delta^{\mu\nu}}{4}q^2)q_\mu p_\nu \times \frac{1}{2}\delta^{\rho\sigma}q_\rho p_\sigma \\ 2(q^\mu q^\nu - \frac{\delta^{\mu\nu}}{4}q^2)q_\mu p_\nu \times \frac{1}{2}\delta^{\rho\sigma}q_\rho p_\sigma & \frac{1}{2}\delta^{\mu\nu}q_\mu p_\nu \times \frac{1}{2}\delta^{\rho\sigma}q_\rho p_\sigma \end{pmatrix} \\
&\to \frac{Z_\phi^2}{M_P^2}\Omega\frac{p^2}{16}\begin{pmatrix} 9q^6 & 3q^4 \\ 3q^4 & q^2 \end{pmatrix},
\end{aligned}
\tag{D31}
$$

where in the last step, we symmetrized loop momenta by $q^\mu q^\nu \to \frac{q^2}{4}\delta^{\mu\nu}$.

Continuing the evaluation of Eq. (D30), the scalar modes in the metric fluctuations gives

$$
\begin{aligned}
\eta_\phi\Big|^{\text{scalar}}_{\text{sunset}} &= -\frac{1}{Z_\phi}\frac{1}{\Omega}\frac{d}{dp^2}\left(\quad + \quad\right)\Big|_{p^2=0} \\
&= -\frac{1}{Z_\phi}\frac{d}{dp^2}\mathrm{Tr}\left[\frac{1}{Z_\phi(P_k+k^2\tilde{m}_H^2)}\frac{Z_\phi^2}{Z_N}\frac{p^2}{16}\begin{pmatrix}9q^6 & 3q^4\\ 3q^4 & q^2\end{pmatrix}\left[\tilde{\mathcal{K}}^{-1}\partial_t\mathcal{R}_k\tilde{\mathcal{K}}^{-1}\right]_{2\times2}\right. \\
&\quad \left. -\frac{1}{Z_\phi}\frac{d}{dp^2}\mathrm{Tr}\left[\frac{\partial_t(Z_\phi R_k)}{Z_\phi^2(P_k+k^2\tilde{m}_H^2)^2}\frac{Z_\phi^2}{Z_N}\frac{p^2}{16}\begin{pmatrix}9q^6 & 3q^4\\ 3q^4 & q^2\end{pmatrix}\tilde{\mathcal{K}}^{-1}\Big|_{2\times2}\right]\right. \\
&= \frac{2}{(4\pi)^2}\frac{4(3-\tilde{\alpha})}{(3-\beta)^2\tilde{M}_P^2}\left[\ell_0^2(\tilde{m}_H^2)\left(\ell_1^6(-\tilde{m}_s^2)+\frac{18(\tilde{\alpha}-\beta)}{(3-\tilde{\alpha})}\left(\ell_1^8(-\tilde{m}_s^2)+\ell_0^8(-\tilde{m}_s^2)\right)\right.\right. \\
&\quad \left. +\frac{108(\tilde{\alpha}-\beta)^2}{(3-\tilde{\alpha})^2}\left(\ell_1^{10}(-\tilde{m}_s^2)+2\ell_0^{10}(-\tilde{m}_s^2)\right)-\frac{108\tilde{\alpha}(3-\beta)^2}{(3-\tilde{\alpha})^2}\ell_0^{10}(0)\right) \\
&\quad +\ell_1^2(\tilde{m}_H^2)\left(\left(1-\tfrac{\eta_\phi}{8}\right)\ell_0^6(-\tilde{m}_s^2)+\left(1-\tfrac{\eta_\phi}{10}\right)\frac{18(\tilde{\alpha}-\beta)}{(3-\tilde{\alpha})}\ell_0^8(-\tilde{m}_s^2)\right. \\
&\quad \left.\left. +\left(1-\tfrac{\eta_\phi}{12}\right)\left(\frac{108(\tilde{\alpha}-\beta)^2}{(3-\tilde{\alpha})^2}\ell_0^{10}(-\tilde{m}_s^2)-\frac{36\tilde{\alpha}(3-\beta)^2}{(3-\tilde{\alpha})^2}\ell_0^{10}(0)\right)\right)\right].
\end{aligned}
\tag{D32}
$$

The total contributions from sunset diagrams to the anomalous dimension of the scalar field is the sum of Eqs. (D28) and (D32).

[1] K. G. Wilson and J. B. Kogut, The renormalization group and the epsilon expansion, Phys. Rep. **12**, 75 (1974).
[2] F. J. Wegner and A. Houghton, Renormalization group equation for critical phenomena, Phys. Rev. A **8**, 401 (1973).
[3] J. Polchinski, Renormalization and effective lagrangians, Nucl. Phys. **B231**, 269 (1984).
[4] C. Wetterich, Exact evolution equation for the effective potential, Phys. Lett. B **301**, 90 (1993).
[5] T. R. Morris, The exact renormalization group and approximate solutions, Int. J. Mod. Phys. A **09**, 2411 (1994).
[6] U. Ellwanger, Flow equations for N point functions and bound states, Z. Phys. C **62**, 503 (1994).
[7] T. R. Morris, Elements of the continuous renormalization group, Prog. Theor. Phys. Suppl. **131**, 395 (1998).
[8] J. Berges, N. Tetradis, and C. Wetterich, Nonperturbative renormalization flow in quantum field theory and statistical physics, Phys. Rep. **363**, 223 (2002).
[9] K. Aoki, Introduction to the nonperturbative renormalization group and its recent applications, Int. J. Mod. Phys. B **14**, 1249 (2000).
[10] C. Bagnuls and C. Bervillier, Exact renormalization group equations. An Introductory review, Phys. Rep. **348**, 91 (2001).
[11] J. Polonyi, Lectures on the functional renormalization group method, Central Eur. J. Phys. **1**, 1 (2003).
[12] J. M. Pawlowski, Aspects of the functional renormalisation group, Ann. Phys. (Amsterdam) **322**, 2831 (2007).
[13] H. Gies, Introduction to the functional RG and applications to gauge theories, Lect. Notes Phys. **852**, 287 (2012).
[14] B. Delamotte, An Introduction to the nonperturbative renormalization group, Lect. Notes Phys. **852**, 49 (2012).
[15] O. J. Rosten, Fundamentals of the exact renormalization group, Phys. Rep. **511**, 177 (2012).
[16] J. Braun, Fermion interactions and universal behavior in strongly interacting theories, J. Phys. G **39**, 033001 (2012).
[17] N. Dupuis, L. Canet, A. Eichhorn, W. Metzner, J. M. Pawlowski, M. Tissier, and N. Wschebor, The nonperturbative functional renormalization group and its applications, Phys. Rep. **910**, 1 (2021).
[18] M. Reuter and C. Wetterich, Effective average action for gauge theories and exact evolution equations, Nucl. Phys. **B417**, 181 (1994).

[19] M. Reuter, Effective average actions and nonperturbative evolution equations, in *Proceedings of the 5th Hellenic School and Workshops on Elementary Particle Physics* (1996).
[20] H. Gies, Running coupling in Yang-Mills theory: A flow equation study, Phys. Rev. D **66**, 025006 (2002).
[21] H. Gies, Renormalizability of gauge theories in extra dimensions, Phys. Rev. D **68**, 085015 (2003).
[22] J. Braun, L. Fister, J. M. Pawlowski, and F. Rennecke, From quarks and gluons to hadrons: Chiral symmetry breaking in dynamical QCD, Phys. Rev. D **94**, 034016 (2016).
[23] M. Mitter, J. M. Pawlowski, and N. Strodthoff, Chiral symmetry breaking in continuum QCD, Phys. Rev. D **91**, 054035 (2015).
[24] A. K. Cyrol, L. Fister, M. Mitter, J. M. Pawlowski, and N. Strodthoff, Landau gauge Yang-Mills correlation functions, Phys. Rev. D **94**, 054005 (2016).
[25] A. K. Cyrol, M. Mitter, J. M. Pawlowski, and N. Strodthoff, Nonperturbative quark, gluon, and meson correlators of unquenched QCD, Phys. Rev. D **97**, 054006 (2018).
[26] L. Corell, A. K. Cyrol, M. Mitter, J. M. Pawlowski, and N. Strodthoff, Correlation functions of three-dimensional Yang-Mills theory from the FRG, SciPost Phys. **5**, 066 (2018).
[27] S. Weinberg, Ultraviolet divergences in quantum theories of gravitation, in *General Relativity: An Einstein Centenary Survey*, edited by S. W. Hawking and W. Israel (Cambridge University Press, Cambridge, England, 1979), Chap. 16.
[28] M. Reuter, Nonperturbative evolution equation for quantum gravity, Phys. Rev. D **57**, 971 (1998).
[29] W. Souma, Nontrivial ultraviolet fixed point in quantum gravity, Prog. Theor. Phys. **102**, 181 (1999).
[30] M. Niedermaier and M. Reuter, The asymptotic safety scenario in quantum gravity, Living Rev. Relativity **9**, 5 (2006).
[31] M. Niedermaier, The asymptotic safety scenario in quantum gravity: An introduction, Classical Quantum Gravity **24**, R171 (2007).
[32] R. Percacci, Asymptotic safety, arXiv:0709.3851.
[33] M. Reuter and F. Saueressig, Quantum Einstein gravity, New J. Phys. **14**, 055022 (2012).
[34] A. Codello, R. Percacci, and C. Rahmede, Investigating the ultraviolet properties of gravity with a Wilsonian renormalization group equation, Ann. Phys. (Amsterdam) **324**, 414 (2009).
[35] A. Eichhorn, Status of the asymptotic safety paradigm for quantum gravity and matter, Found. Phys. **48**, 1407 (2018).
[36] R. Percacci, *An Introduction to Covariant Quantum Gravity and Asymptotic Safety*, 100 Years of General Relativity.World Scientific Vol. 3 (World Scientific Publishing, Singapore, 2017).
[37] A. Eichhorn, An asymptotically safe guide to quantum gravity and matter, Front. Astron. Space Sci. **5**, 47 (2019).
[38] M. Reuter and F. Saueressig, *Quantum Gravity and the Functional Renormalization Group: The Road towards Asymptotic Safety* (Cambridge University Press, Cambridge, England, 2019).
[39] C. Wetterich, Quantum scale symmetry, arXiv:1901.04741.
[40] A. Bonanno, A. Eichhorn, H. Gies, J. M. Pawlowski, R. Percacci, M. Reuter, F. Saueressig, and G. P. Vacca, Critical reflections on asymptotically safe gravity, Front. Phys. **8**, 269 (2020).
[41] M. Reichert, Lecture notes: Functional renormalisation group and asymptotically safe quantum gravity, *Proc. Sci.*, Modave2019 (2020) 005.
[42] J. M. Pawlowski and M. Reichert, Quantum gravity: A fluctuating point of view, Front. Phys. **8**, 527 (2021).
[43] P. M. Stevenson, Optimized perturbation theory, Phys. Rev. D **23**, 2916 (1981).
[44] R. D. Ball, P. E. Haagensen, J. I. Latorre, and E. Moreno, Scheme independence and the exact renormalization group, Phys. Lett. B **347**, 80 (1995).
[45] H. Gies, B. Knorr, and S. Lippoldt, Generalized parametrization dependence in quantum gravity, Phys. Rev. D **92**, 084020 (2015).
[46] R. Percacci and D. Perini, Asymptotic safety of gravity coupled to matter, Phys. Rev. D **68**, 044018 (2003).
[47] G. Narain and R. Percacci, Renormalization group flow in scalar-tensor theories. I, Classical Quantum Gravity **27**, 075001 (2010).
[48] G. Narain and C. Rahmede, Renormalization group flow in scalar-tensor theories. II, Classical Quantum Gravity **27**, 075002 (2010).
[49] R. Percacci and G. P. Vacca, Search of scaling solutions in scalar-tensor gravity, Eur. Phys. J. C **75**, 188 (2015).
[50] K.-Y. Oda and M. Yamada, Non-minimal coupling in Higgs-Yukawa model with asymptotically safe gravity, Classical Quantum Gravity **33**, 125011 (2016).
[51] P. Labus, R. Percacci, and G. P. Vacca, Asymptotic safety in $O(N)$ scalar models coupled to gravity, Phys. Lett. B **753**, 274 (2016).
[52] Y. Hamada and M. Yamada, Asymptotic safety of higher derivative quantum gravity non-minimally coupled with a matter system, J. High Energy Phys. 08 (2017) 070.
[53] A. Eichhorn, Y. Hamada, J. Lumma, and M. Yamada, Quantum gravity fluctuations flatten the Planck-scale Higgs potential, Phys. Rev. D **97**, 086004 (2018).
[54] J. M. Pawlowski, M. Reichert, C. Wetterich, and M. Yamada, Higgs scalar potential in asymptotically safe quantum gravity, Phys. Rev. D **99**, 086010 (2019).
[55] C. Wetterich and M. Yamada, Variable Planck mass from the gauge invariant flow equation, Phys. Rev. D **100**, 066017 (2019).
[56] M. Shaposhnikov and C. Wetterich, Asymptotic safety of gravity and the Higgs boson mass, Phys. Lett. B **683**, 196 (2010).
[57] A. Eichhorn and A. Held, Viability of quantum-gravity induced ultraviolet completions for matter, Phys. Rev. D **96**, 086025 (2017).
[58] A. Eichhorn and A. Held, Top mass from asymptotic safety, Phys. Lett. B **777**, 217 (2018).
[59] A. Eichhorn and A. Held, Mass Difference for Charged Quarks from Asymptotically Safe Quantum Gravity, Phys. Rev. Lett. **121**, 151302 (2018).
[60] R. Alkofer, A. Eichhorn, A. Held, C. M. Nieto, R. Percacci, and M. Schröfl, Quark masses and mixings in minimally parameterized UV completions of the Standard Model, Ann. Phys. (Amsterdam) **421**, 168282 (2020).

[61] C. Wetterich and M. Yamada, Gauge hierarchy problem in asymptotically safe gravity–the resurgence mechanism, Phys. Lett. B **770**, 268 (2017).
[62] A. Codello and R. Percacci, Fixed Points of Higher Derivative Gravity, Phys. Rev. Lett. **97**, 221301 (2006).
[63] D. Benedetti, P. F. Machado, and F. Saueressig, Asymptotic safety in higherderivative gravity, Mod. Phys. Lett. A **24**, 2233 (2009).
[64] D. Benedetti, P. F. Machado, and F. Saueressig, Taming perturbative divergences in asymptotically safe gravity, Nucl. Phys. **B824**, 168 (2010).
[65] N. Ohta and R. Percacci, Higher derivative gravity and asymptotic safety in diverse dimensions, Classical Quantum Gravity **31**, 015024 (2014).
[66] N. Ohta and R. Percacci, Ultraviolet fixed points in conformal gravity and general quadratic theories, Classical Quantum Gravity **33**, 035001 (2016).
[67] D. Benedetti, On the number of relevant operators in asymptotically safe gravity, Europhys. Lett. **102**, 20007 (2013).
[68] K. Falls, D. F. Litim, K. Nikolakopoulos, and C. Rahmede, A bootstrap towards asymptotic safety, arXiv:1301.4191.
[69] K. Falls, D. F. Litim, K. Nikolakopoulos, and C. Rahmede, Further evidence for asymptotic safety of quantum gravity, Phys. Rev. D **93**, 104022 (2016).
[70] K. Falls, C. R. King, D. F. Litim, K. Nikolakopoulos, and C. Rahmede, Asymptotic safety of quantum gravity beyond Ricci scalars, Phys. Rev. D **97**, 086006 (2018).
[71] K. G. Falls, D. F. Litim, and J. Schröder, Aspects of asymptotic safety for quantum gravity, Phys. Rev. D **99**, 126015 (2019).
[72] K. Falls, N. Ohta, and R. Percacci, Towards the determination of the dimension of the critical surface in asymptotically safe gravity, Phys. Lett. B **810**, 135773 (2020).
[73] Y. Kluth and D. F. Litim, Fixed points of quantum gravity and the dimensionality of the UV critical surface, arXiv:2008.09181.
[74] M. Reichert and J. Smirnov, Dark matter meets quantum gravity, Phys. Rev. D **101**, 063015 (2020).
[75] Y. Hamada, K. Tsumura, and M. Yamada, Scalegenesis and fermionic dark matters in the flatland scenario, Eur. Phys. J. C **80**, 368 (2020).
[76] K. Kowalska and E. M. Sessolo, Minimal models for g-2 and dark matter confront asymptotic safety, Phys. Rev. D **103**, 115032 (2021).
[77] A. Eichhorn and M. Pauly, Safety in darkness: Higgs portal to simple Yukawa systems, Phys. Lett. B **819**, 136455 (2021).
[78] A. Eichhorn and M. Pauly, Constraining power of asymptotic safety for scalar fields, Phys. Rev. D **103**, 026006 (2021).
[79] A. Eichhorn, M. Pauly, and S. Ray, Towards a Higgs mass determination in asymptotically safe gravity with a dark portal, J. High Energy Phys. 10 (2021) 100.
[80] A. Eichhorn, A. Held, and C. Wetterich, Quantum-gravity predictions for the fine-structure constant, Phys. Lett. B **782**, 198 (2018).
[81] G. P. De Brito, Y. Hamada, A. D. Pereira, and M. Yamada, On the impact of Majorana masses in gravity-matter systems, J. High Energy Phys. 08 (2019) 142.
[82] K. Kowalska, E. M. Sessolo, and Y. Yamamoto, Flavor anomalies from asymptotically safe gravity, Eur. Phys. J. C **81**, 272 (2021).
[83] S. Falkenberg and S. D. Odintsov, Gauge dependence of the effective average action in Einstein gravity, Int. J. Mod. Phys. A **13**, 607 (1998).
[84] W. Souma, Gauge and cutoff function dependence of the ultraviolet fixed point in quantum gravity, arXiv:gr-qc/0006008.
[85] V. F. Barra, P. M. Lavrov, E. A. Dos Reis, T. de Paula Netto, and I. L. Shapiro, Functional renormalization group approach and gauge dependence in gravity theories, Phys. Rev. D **101**, 065001 (2020).
[86] H. Kawai, Y. Kitazawa, and M. Ninomiya, Scaling exponents in quantum gravity near two-dimensions, Nucl. Phys. **B393**, 280 (1993).
[87] N. Ohta, R. Percacci, and G. P. Vacca, Flow equation for $f(R)$ gravity and some of its exact solutions, Phys. Rev. D **92**, 061501 (2015).
[88] N. Ohta, R. Percacci, and G. P. Vacca, Renormalization group equation and scaling solutions for $f(R)$ gravity in exponential parametrization, Eur. Phys. J. C **76**, 46 (2016).
[89] K. Falls and N. Ohta, Renormalization group equation for $f(R)$ gravity on hyperbolic spaces, Phys. Rev. D **94**, 084005 (2016).
[90] N. Ohta, R. Percacci, and A. D. Pereira, Gauges and functional measures in quantum gravity I: Einstein theory, J. High Energy Phys. 06 (2016) 115.
[91] N. Ohta, R. Percacci, and A. D. Pereira, Gauges and functional measures in quantum gravity II: Higher derivative gravity, Eur. Phys. J. C **77**, 611 (2017).
[92] G. P. De Brito, N. Ohta, A. D. Pereira, A. A. Tomaz, and M. Yamada, Asymptotic safety and field parametrization dependence in the $f(R)$ truncation, Phys. Rev. D **98**, 026027 (2018).
[93] J. D. Gonçalves, T. de Paula Netto, and I. L. Shapiro, Gauge and parametrization ambiguity in quantum gravity, Phys. Rev. D **97**, 026015 (2018).
[94] A. Nink, Field parametrization dependence in asymptotically safe quantum gravity, Phys. Rev. D **91**, 044030 (2015).
[95] K. Falls, Renormalization of Newton's constant, Phys. Rev. D **92**, 124057 (2015).
[96] C. Wetterich, Quantum correlations for the metric, Phys. Rev. D **95**, 123525 (2017).
[97] C. Wetterich, Gauge invariant flow equation, Nucl. Phys. **B931**, 262 (2018).
[98] D. F. Litim, Optimized renormalization group flows, Phys. Rev. D **64**, 105007 (2001).
[99] C. Wetterich, Graviton fluctuations erase the cosmological constant, Phys. Lett. B **773**, 6 (2017).
[100] C. Wetterich, Infrared limit of quantum gravity, Phys. Rev. D **98**, 026028 (2018).
[101] K.-I. Aoki and D. Sato, Solving the QCD non-perturbative flow equation as a partial differential equation and its application to the dynamical chiral symmetry breaking, Prog. Theor. Exp. Phys. **2013**, 043B04 (2013).

[102] L. Bosma, B. Knorr, and F. Saueressig, Resolving Spacetime Singularities within Asymptotic Safety, Phys. Rev. Lett. **123**, 101301 (2019).
[103] B. Knorr, C. Ripken, and F. Saueressig, Form factors in asymptotic safety: Conceptual ideas and computational toolbox, Classical Quantum Gravity **36**, 234001 (2019).
[104] A. Bonanno, T. Denz, J. M. Pawlowski, and M. Reichert, Reconstructing the graviton, arXiv:2102.02217.
[105] B. Knorr and M. Schiffer, Non-perturbative propagators in quantum gravity, Universe **7**, 216 (2021).
[106] N. Christiansen, D. F. Litim, J. M. Pawlowski, and A. Rodigast, Fixed points and infrared completion of quantum gravity, Phys. Lett. B **728**, 114 (2014).
[107] N. Christiansen, B. Knorr, J. M. Pawlowski, and A. Rodigast, Global flows in quantum gravity, Phys. Rev. D **93**, 044036 (2016).
[108] N. Christiansen, B. Knorr, J. Meibohm, J. M. Pawlowski, and M. Reichert, Local quantum gravity, Phys. Rev. D **92**, 121501 (2015).
[109] J. Meibohm and J. M. Pawlowski, Chiral fermions in asymptotically safe quantum gravity, Eur. Phys. J. C **76**, 285 (2016).
[110] N. Christiansen, Four-derivative quantum gravity beyond perturbation theory, arXiv:1612.06223.
[111] T. Denz, J. M. Pawlowski, and M. Reichert, Towards apparent convergence in asymptotically safe quantum gravity, Eur. Phys. J. C **78**, 336 (2018).
[112] N. Christiansen, D. F. Litim, J. M. Pawlowski, and M. Reichert, Asymptotic safety of gravity with matter, Phys. Rev. D **97**, 106012 (2018).
[113] N. Christiansen, K. Falls, J. M. Pawlowski, and M. Reichert, Curvature dependence of quantum gravity, Phys. Rev. D **97**, 046007 (2018).
[114] A. Eichhorn, P. Labus, J. M. Pawlowski, and M. Reichert, Effective universality in quantum gravity, SciPost Phys. **5**, 031 (2018).
[115] A. Eichhorn, S. Lippoldt, J. M. Pawlowski, M. Reichert, and M. Schiffer, How perturbative is quantum gravity?, Phys. Lett. B **792**, 310 (2019).